



United States Department of Commerce
National Institute of Standards and Technology

NISTIR 3967

Report No. 22

TREAD CRACK DETECTION IN RAILROAD WHEELS: AN ULTRASONIC SYSTEM USING EMATS

Raymond E. Schramm
Alfred V. Clark, Jr.
Dragan V. Mitraković
Yossef Cohen
Peter J. Schull
Stephen R. Schaps

Report No. 22

TREAD CRACK DETECTION IN RAILROAD WHEELS: AN ULTRASONIC SYSTEM USING EMATS

Raymond E. Schramm

Alfred V. Clark, Jr.

Dragan V. Mitraković*

Yossef Cohen**

Peter J. Schull***

Stephen R. Schaps

Materials Reliability Division

Materials Science and Engineering Laboratory

National Institute of Standards and Technology

Boulder, Colorado 80303-3328

*NIST Guest Researcher, on leave from the University of Belgrade

**NIST Guest Researcher, on leave from the Nuclear Research Center – Negev, Beer Sheva Israel

***Present address: Dept. of Materials Science, Johns Hopkins Univ., Baltimore, Maryland

May 1991

Prepared for

U.S. Department of Transportation

Federal Railroad Administration

Office of Research and Development

Washington, DC 20590



U.S. DEPARTMENT OF COMMERCE, Robert A. Mosbacher, Secretary

NATIONAL INSTITUTE OF STANDARDS AND TECHNOLOGY, John W. Lyons, Director

CONTENTS

	Page
ABSTRACT	1
INTRODUCTION	2
CONTRACT HISTORY	3
WHEEL INSPECTION SYSTEMS: OVERVIEW	
Conventional Ultrasonics	4
EMAT Ultrasonics - Germany	5
EMAT Ultrasonics - United States	5
Magnetic	5
References	6
IN-RAIL EMATS	
Principles	9
Configuration	11
OPERATIONAL PRINCIPLES	
Transducer Package	14
Analog Electronics	18
Digital Electronics	18
Report Station	18
EQUIPMENT INSTALLATION	
In-Track EMAT	18
Connections and Cables	21
EXPERIMENTAL RESULTS	23
Laboratory Tests	23
Acoustic Signatures	23
Wheel OK	23
Single Flaw	26
Multiple Flaws	26
Blind Spots	26
Field Tests	27
ELECTRONIC SCHEMATICS	
Analog	28
Digital	31
List of Electronic Components	31
SOFTWARE	
Operation	47
Program Listings	48
CHECKLIST	60
TROUBLE SHOOTING	60
FUTURE CONSIDERATIONS	61
OTHER POTENTIAL APPLICATIONS	63
ACKNOWLEDGMENTS	63
APPENDIX: PUBLIC NOTICES	64

TREAD CRACK DETECTION IN RAILROAD WHEELS:
AN ULTRASONIC SYSTEM USING EMATS

Raymond E. Schramm, Alfred V. Clark, Jr.,
Dragan V. Mitrakovic,^{*} Yossef Cohen,^{**}
Peter J. Shull,^{***} and Stephen R. Schaps

Materials Reliability Division
Materials Science and Engineering Laboratory
National Institute of Standards and Technology
Boulder, Colorado 80303-3328

* NIST Guest Researcher, on leave from the University of Belgrade

** NIST Guest Researcher, on leave from the Nuclear Research Center -
Negev, Beer Sheva, Israel

*** Present Address: Dept. of Materials Science, Johns Hopkins University,
Baltimore, Maryland

This is report number 22 in a series covering research performed by the National Institute of Standards and Technology (NIST) for the Federal Railroad Administration (FRA). This report covers a project by the Materials Reliability Division (formerly the Fracture and Deformation Division) to develop and build an ultrasonic system to detect crack-type flaws in the tread of railroad wheels. To achieve fully automatic operation, the sensor is built into the rail so testing occurs as the train rolls past. Signal analysis takes place in real time.

The ultrasonic probe is an EMAT (electromagnetic-acoustic transducer). As configured here, the EMAT has a small footprint, and, due to its principle of operation, it does not require any acoustic couplant. The system operates in a pitch-catch mode. A short burst of Rayleigh (surface) waves travels around the wheel tread, and an echo indicates a flaw's presence and size. Testing was performed on both a short track in the NIST laboratory and the full-scale facilities of the Transportation Test Center (TTC) in Pueblo, Colorado.

This report documents the design, construction, and testing of the system. It is also to serve as an operational guide for the equipment being delivered to the FRA.

Key words: crack; EMAT; nondestructive testing; railroad wheel; roll-by inspection; ultrasonic.

INTRODUCTION

In this country, most railroad operations now deal with the transportation of freight in its many forms. Modern needs place ever greater demands on the elaborate rail network that began developing early last century. Just one of the important elements in this complex system is the integrity of the many wheels that bear the loads. As massive as the cast-steel wheels used in the U.S. are, they would not seem to be a problem. Accident statistics, however, indicate otherwise. According to the Accident/Incident Bulletin of the FRA Office of Safety, broken wheels caused 134 accidents in the four year period of 1985-1988, resulting in losses totaling \$27.5M. Besides the direct and indirect cost of such problems, there is the threat to human life and health due to the accidents themselves or the potential environmental impact from the release of dangerous materials. Disruption to commerce at many levels is almost inevitable.

During their lifetime, wheels see a wide variety of sometimes extreme conditions. Among these are large static and dynamic mechanical loads, large-scale frictional wear, high temperatures from braking operations, environmental extremes, and exposure to potentially corrosive materials. All these factors operate to initiate tread cracks or aggravate any existing faults. According to the stress conditions (applied and residual), crack growth can be very slow and gradual or rapid, even explosive. The relative rarity of failures under all these extreme conditions speaks well for the progress made in wheel design and manufacture.

Wheel improvements will continue, but it will not be possible to eliminate completely the tread cracks that may, in the presence of tensile stresses, lead to failure. For economic, environmental, and safety reasons, replacement before failure is the preferred approach. Because of the costs and uncertainties involved, retirement-for-cause is favored, whenever possible, over replacement at predetermined intervals. Effective and efficient nondestructive evaluation makes it possible to evaluate fitness-for-service. For railroad wheels, as in most other applications, the first NDE test is visual examination by a skilled inspector. In practice, however, this simple approach has severe limitations. Some of the problems include: hidden flaws, inability to quantify flaw size, and unfavorable conditions (e.g., position, lighting). The ideal test would be simple, reliable, unintrusive, inexpensive, and operator independent. No available techniques fulfill all these conditions perfectly, but ultrasonic testing offers a possible major step in this direction.

The ultrasonic system examined here follows upon prior efforts at NIST and elsewhere and the experience and expertise with electromagnetic-acoustic transducers in this laboratory. After laboratory testing and development, we built a prototype for delivery to the FRA. This will receive extensive field testing and exposure to potential users. The desired goal is to develop an instrument of value to the railroad industry that private industry would license for commercial production.

The plan for this NDE instrument was to have a sensor placed in a test rail located on the outskirts of a rail yard, or on a dedicated track siding.

The train to be tested would simply roll over the test track (at speeds up to 25 km/h or 16 mph). The testing would be automatic and the report produced at some desired remote site (e.g., the yard office). Maintenance will likely be simple and minimal.

CONTRACT HISTORY

As the Fracture and Deformation Division of the National Bureau of Standards, we first received a Federal Railroad Administration research contract to develop nondestructive evaluation (NDE) procedures for railroad wheels in September 1985. During the period of this work, we have been renamed the Materials Reliability Division of the National Institute of Standards and Technology. Our contract monitors have been M. Clifford Gannett, Claire Orth, and Donald E. Gray. The current contract is Reimbursable Agreement No. DTFR53-89-X-00018 with an effective date of 4/21/89.

Over the past few years, we presented the results of the work done under this sponsorship at five meetings:

1. Review of Progress in Quantitative Nondestructive Evaluation, Williamsburg, Virginia, June 1987.
2. Review of Progress in Quantitative Nondestructive Evaluation, La Jolla, California, August 1988.
3. Nondestructive Testing and Evaluation for Manufacturing and Construction, Urbana, Illinois, August 1988.
4. Third International Symposium on Nondestructive Characterization of Materials, Saarbrücken, Federal Republic of Germany, October 1988.
5. American Society for Nondestructive Testing, fall conference, Seattle, Washington, October 9-12, 1990.

Publications resulting from these conferences are:

1. "Flaw Detection in Railroad Wheels Using Rayleigh-Wave EMATs," R. E. Schramm, A. V. Clark, Jr., D. V. Mitraković, and P. J. Shull in Review of Progress in Quantitative Nondestructive Evaluation, Vol. 7B, D. O. Thompson and D. E. Chimenti, eds., Plenum Press, New York (1988), 1661-1668.
2. "EMAT Examination for Cracks in Railroad Wheel Treads," R. E. Schramm, P. J. Shull, A. V. Clark, Jr., and D. V. Mitraković in Nondestructive Testing and Evaluation for Manufacturing and Construction, Conference proceedings, Urbana, Illinois, Aug. 9-12, 1988, H. L. M. dos Rios, ed., Hemisphere Publishing Corp., new York (1990), 373-380.
3. "EMATs for Roll-By Crack Inspection of Railroad Wheels," R. E. Schramm, P. J. Shull, A. V. Clark, Jr., and D. V. Mitraković in Review of Progress in Quantitative Nondestructive Evaluation, Vol. 8A, D. O. Thompson and D. E. Chimenti, eds., Plenum Press, New York (1989), 1083-1089.

4. "Crack Inspection of Railroad Wheel Treads by EMATs," R. E. Schramm, P. J. Shull, A. V. Clark, Jr., and D. V. Mitraković in Nondestructive Characterization of Materials, Proceedings of the 3rd International Symposium, Saarbrücken, FRG, Oct. 3-6, 1988, P. Höller, V. Hauk, G. Dobmann, C. O. Ruud, and R. E. Green, eds., Springer-Verlag, New York ((1989), 421-428.

Most of this material was collected together and published as:

Report No. 18: Ultrasonic Railroad Wheel Inspection Using EMATs,
Raymond E. Schramm and A. Van Clark, Jr., NISTIR 88-3906, Dec. 1988.

Other work done under this contract focused on the measurement of residual stress in the rim of railroad wheels. The approach has been to use an ultrasonic birefringence method, also based on EMATs. The results of this parallel study are in a subsequent NISTIR 91-3968:

Report No. 23: Residual Stress Detection in Railroad Wheels: An Ultrasonic System Using EMATs.

WHEEL INSPECTION SYSTEMS: OVERVIEW

Conventional Ultrasonics

In the mid-1970's, The Fax Corporation in Connecticut introduced the WHEELFAX* automatic ultrasonic system to examine each wheel as it rolled by a checkpoint in a railyard [1-4]. Their ultrasonic probe, situated inside the rail, is a pair of piezoelectric transducers within a liquid-filled polyurethane boot. To aid the transmission of the probing signal into and back out of the wheel, there are two nozzles spraying fluid onto the tread as it passes. The basic idea, as in many ultrasonic approaches, is to inject high frequency sound and then electronically analyze echoes generated by any flaws present. The concept and engineering of this system are very good, but the device has achieved only limited acceptance. The currently active installations in this country are on a Florida-based railroad. There are also plans for a test at the North Platte, Nebraska, railyard. Two problems seem to have prevented large scale implementation: (1) a very high rate of false positive indications, and (2) fragility, since the boot is very susceptible to small cuts which release the pressurized liquid couplant and disrupt operation. Unfortunately, as wheel treads abrade, wear does develop occasional slivers which are short-lived but very sharp and hazardous. Ongoing developments in electronics and signal processing are improving performance.

* The use of trade names in no way implies endorsement or approval by NIST and is included only for identification.

EMAT Ultrasonics - Germany

For more than ten years, the Fraunhofer Institute for Nondestructive Testing (IzfP, Saarbrücken, Germany) has been working on an ultrasonic inspection system based on the same concept and physics used in the conventional approach, but taking a different approach to the transducers [5-8]. The Germans employ noncontacting electromagnetic-acoustic transducers (EMATs) that do not require an acoustic couplant to the wheel as do the conventional transducers. EMATs simplify the mechanics of the rail mounting (since they are generally smaller and more compact), cut the number of false positives (since they have a purer mode of operation and eliminate many extraneous interfaces in the signal path), and should be more durable (since there is no pressurized rubber boot). A few years ago IzfP installed a prototype system in Wuerzburg for use on the high-speed German experimental Intercity Express (ICE). This system has now been relocated to Hamburg.

EMAT Ultrasonics - United States

The IzfP system inspects a small number of forged wheels on passenger cars and locomotives; these wheels all have tightly controlled wear profiles required of high-speed passenger traffic. In our current project, NIST seeks to use EMATs to inspect cast wheels on long freight trains which will generally have a variety of tread wear patterns and damage states. The major differences between German and U.S. applications of roll-by inspection systems have led us to incorporate several major variations:

1. In-rail transducer configuration to accommodate various wheel profiles.
2. Use of a permanent magnet instead of an electromagnet to allow operation on long trains.
3. Real-time, rather than off-line, signal processing for use in heavy traffic situations.

Magnetic

One other method has been proposed. Instead of an ultrasonic probe, this system from Wheel Checkers in Colorado passes a thin steel tape past the tread of the moving wheel [9]. This tape carries a continuous recorded tone and the wheel is subjected to a strong magnetic field. Any perturbation in the surface (i.e., a crack) will introduce a magnetic field gradient which will distort the tone on the tape. This method has not received a field trial, but the equipment is currently at the Transportation Test Center in Pueblo, Colorado.

The following table contains some brief notes comparing the previous ultrasonic systems with the one we have been developing.

References

- [1] Inspect Wheels "In Motion," Progressive Railroading, Jan. 1974.
- [2] Spotting the Defects in Railroad Wheels, Business Week, p. 44, Sept. 28, 1974.
- [3] Cracked-Wheel Detector "Could Save Millions," Railway Systems Control, May 1975.
- [4] U.S. Patent 3,812,708: May 28, 1974, John Vincent Cowan, Gerald DeG. Cowan, and John Gerald Cowan.
- [5] Salzburger, H. J., and Repplinger, W., Ultrasonics International 83, conference organizers Z. Novak and S. L. Bailey (Butterworth & Co. Ltd., Kent, Great Britain), pp. 8-12, 1983.
- [6] Salzburger, H. J., Repplinger, W., and Schmidt, W., Deutsche Gesellschaft für zerstörungsfreie Prüfung, Jahrestagung 25, Berichtsband 10, Teil 1, pp.51-60, 1987.
- [7] Salzburger, H. J., and Schmidt, W., Mit vernetzten, intelligenten Komponenten zu leistungsfähigeren Mess- und Automatisierungssystemen, München, Oldenbourg, pp. 124-133, 1989.
- [8] German Patent OS DE 3505260 A1: Ultraschall-Prüfvorrichtung zur zerstörungsfreien Prüfung der Lauffläche von Schienenfahrzeugräder Anmelder: Deutsche Bundesbahn.
- [9] U.S. Patent 3,820,016: June 25, 1974, Marion W. Gieskieng.

Comparisons of In-Rail Ultrasonic Systems

	WHeeLFAX	IzfP	NIST
Sensors, transducers (Rayleigh wave)	Piezoelectric (2), sequential fire (if time is available), unidirectional	EMAT using electromagnet, 2 tandem serpentine coils of 4 cycles, approx. 24 random wire turns, bidirectional	EMAT using permanent magnet, 2 overlapping serpentine coils of 7 ordered wire turns, bidirectional
Frequency	400 kHz	450 kHz	500 kHz
Wheel trigger	Pressure sensor at bottom of fluid-filled boot	Inductive pickup	Membrane switch operated by pressure through foam pad
Wheel contact (in rail)	Polyurethane boot filled with antifreeze, tread sprayed with detergent solution, acoustic contact through flexible boot to wet wheel	Rigid assembly pivots as wheel passes over	Flexible cover and coils (over foam) conform to wheel profile, magnet rigidly mounted inside rail
Footprint, rail cut out	2½" x 5" wheel contact -- cut out = full rail head width x full rail head depth x approx. 8" length -- needs additional rail for weight bearing	Larger than NIST cut out	1½" x 3½" wheel contact -- cut out is full rail head depth (slight penetration into rail web) -- remaining rail head width is sufficient for weight bearing (needs no additional support)
Analog signal	Detected, log amplified	Detected, log amplified	Detected, log amplified
Signal processing	Digitize for approx. 2 ms, find peaks, extrapolate to time=0 (remove attenuation), flaw signal = amplitude ratio of 1st echo to 1st round trip, near real time	Digitize & find peaks, flaw signal = amplitude ratio of 1st echo to 1st round trip, offline processing	Peak detect for approx. 2 ms, peaks digitized, flaw signal = amplitude ratio of 1st echo to 1st round trip, near real time

Continued

Continued

	WHeeLFAX	IzfP	NIST
Output -- signals and flags	1.critical flaw (amplitude ratio adjustable) 2.no test 3.wheel size	1.critical flaw (users set amplitude ratio empirically)	1.critical flaw (amplitude ratio adjustable) 2.too many flaws(>3) 3."poor" metal (high attenuation, no 2nd round trip) 4.no test 5.wheel size
Cables, connectors	Twisted pair, screw terminals	Twinax and/or Lemo connectors	Coax RG58C/U (3 @ 10 m long) with BNC's
Installations	Jacksonville and Hialeah, FL, on Florida East Coast Railroad - test site in North Platte, NE for UP	Part of test facility for ICE (InterCity Express) of the Deutsche Bundesbahn - now in Hamburg	Field tests at TTC, Pueblo, CO
History	Patent in 1974	Installed 1987, approx. 10 yrs. development, German patent	Began research in 1985, 1st field test in 1989, prototype delivery in 1991
Equipment location	Pulser and preamp at trackside, processing in hut 20 m away, report at yard office 2.5 km away (by fiberoptic link)	Analog electronics probably at track side	10 m of cable to analog and digital electronics, report can be remote
Guide rail	Yes	No?	Probably not
Service required at track	Boot needs replacement, filling, and bleeding when slit; need to refill spray tank	None	Replace coil package after wear (aim for >1 week intervals) - requires 2 nuts and 3 BNC connectors (approx. 5 min.)
Problems			Collection of magnetic dust at EMAT, coil package durability, weatherization

IN-RAIL EMATS

EMATs (electromagnetic-acoustic transducers) are devices that generate and detect sound energy directly in an electrically conductive specimen. A major advantage of these devices is that they do not require the acoustic couplants usually associated with piezoelectric transducers. This simplifies operation and eliminates echoes and mode conversions that might occur at the interfaces the signal would otherwise have to traverse. Furthermore, they can operate effectively on rough and pitted surfaces.

Principles

To indicate basic EMAT operation, Fig. 1 shows a primitive element composed of a wire conductor carrying a dynamic current I_ω and a source of strong magnetic field H_0 . The current I_ω induces dynamic eddy currents J_ω in the metal conductor surface. H_0 causes the deflection of the moving electrons in a direction defined by $J_\omega \times H_0$. The resultant Lorentz body forces, T , generate ultrasonic signals that propagate radially into the specimen.

The polarization and propagation direction of an ultrasonic wave from an EMAT are the result of the orientation of the electric and magnetic fields and the arrangement of the primitive elements. For the examination of the wheel tread, we want a Rayleigh wave, one that travels along the surface and does not penetrate into the bulk of the wheel. To generate this ultrasonic signal, a coil with a serpentine layout is necessary (Fig. 2). The periodicity of the coil is the wavelength of the surface wave, in this instance, 6 mm at 500 kHz. Repetition of the windings increases the ampere-turns of the transducer for best signal strength. A flexible substrate and support allows the coils to conform to the wheel's curvature for greatest efficiency. This coil is currently laid out by hand, but automatic production is available for large quantities.

Separate transmitter and receiver EMATs are usually physically separated and each has its own magnet. We found we could minimize the size of the cutout

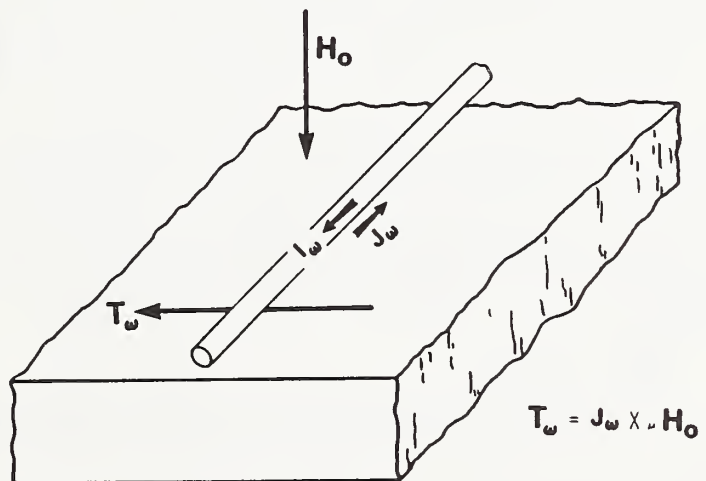


Figure 1. Primitive EMAT element.

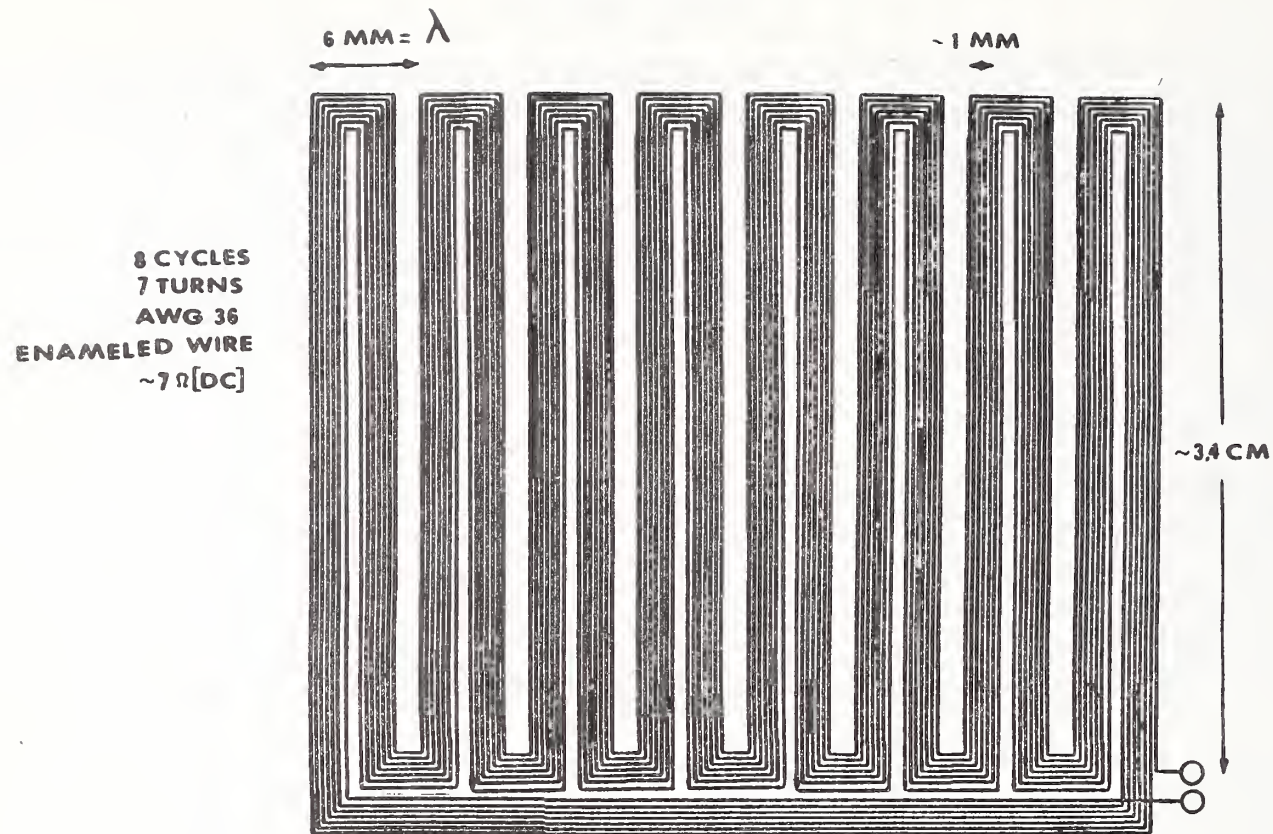


Figure 2. Schematic of the EMAT coils used to generate and receive Rayleigh waves. A flexible substrate allows them to conform to the curvature of the wheel.

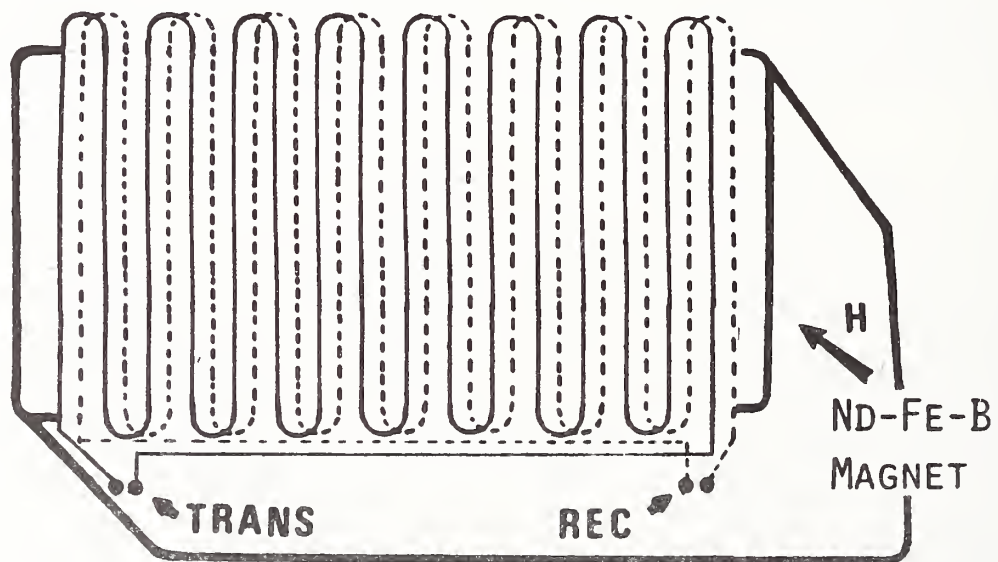


Figure 3. Compact configuration of transmitter and receiver coils relative to the magnet. The shift between the coils minimizes the mutual shielding.

in the rail by stacking two of these serpentine coils and using only one magnet. Careful staggering so that the wire legs of one coil show through the open area of the other coil reduces the problem of mutual shielding. Figure 3 indicates this arrangement, and the compact configuration that results.

While EMATs cannot operate efficiently at large liftoffs (distance to the workpiece), they can generally tolerate a separation on the order of millimeters, and this is sufficient for roll-by inspection. Another EMAT advantage is its high degree of selectivity, an ability to reject most signals with an undesired polarization. This means a simpler echo pattern and less confusion in data interpretation. In all the work of interest here, the signal is a Rayleigh (surface) wave which travels around the outer tread of the wheel and does not penetrate into the surface very far (≈ 10 mm, in this case).

During the course of field tests, various factors, such as loading, fatigue, penetration of fine sand through the covering, etc., have caused the coil windings to deviate noticeably from their original neat and symmetric pattern (Fig. 2). In spite of these deformations, the signal strength did not appear to diminish. The nature of the induction mechanisms and the operational frequency contribute to a considerable robustness in use.

Configuration

During our laboratory research, the in-rail transducer evolved into a two-part device, magnet and coil package, mounted inside a test rail 2 m long.

The magnet here is a 52 mm \times 26 mm \times 31 mm block of Nd-Fe-B with a nominal energy product of 0.28 MJ/m³ (35 MG·Oe). The field direction is along the 31 mm dimension and must be vertical in the track. A copper box surrounds it, permitting mechanical attachment to the rail and shielding the magnet from eddy currents generated by the coils. The exact configuration of this box is not critical, but Fig. 4 gives some idea of the construction used here. The copper is 0.8 mm (1/32 in) thick sheet cut into two sections. Each surrounds three sides of the magnet and has ears extending from both ends. The 1/4-20 bolts in the test rail pass through slots in the ears and hold the magnet firmly in its pocket.

The coil package is a complex structure mounted on a bracket of aluminum sheet 1.6 mm thick (Fig. 5). The vertical plate (approximately 100 mm square) has two slotted holes for bolting to the rail head and holes for the BNC connectors. The horizontal plate (approximately 40 mm \times 80 mm) is the support platform for two coils and the trigger switches.

The bottom layer is a pad of six membrane switches (Fig. 6) used to trigger the electronics when a wheel is in position. The current connection of these switches allows for setting up two independent systems. Until it is determined that one configuration is better than the other, they can be considered redundant. Trigger 1 is a pair of OR gates, right and left, connected to make them an AND gate. The trigger occurs with the closure of

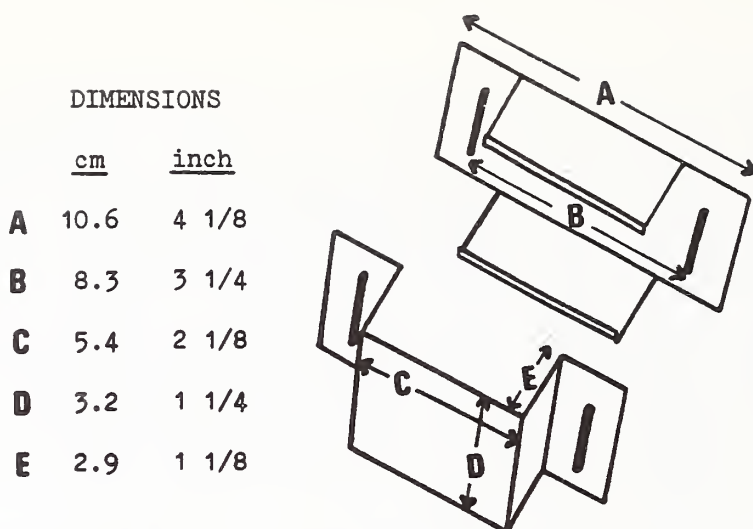


Figure 4. Sketch of copper box (two pieces) holding the magnet in the rail pocket. The slots in the ears match the bolts in the test rail. The magnetic field must be vertical (D direction).

either switch on the left and either switch on the right. Trigger 2 is simply a pair of OR gates; the trigger occurs when either switch is closed. There are independent connections to the two systems.

Over the switches is a 5 mm thickness of resilient foam with small, closed cells. This material has two functions. First, it compresses under the load of the passing wheel and presses the flexible coils into the tread profile. This close coupling insures the maximum signal amplitude. Second, the foam transmits pressure to close the membrane switches under it.

Atop the foam is a thin (0.5 mm) sheet of fiberglass/epoxy composite. While this material will flex to the wheel curvature, it provides mechanical support for the coils and prolongs their fatigue life. Perhaps more importantly, it supports the coil electrical connection, which have, so far, proven to be the most fragile part of this package.

The two EMAT coils are on the top of this support sheet. They are shifted with respect to each other, as noted above (Fig. 3), and fixed into position.

Next is a thick (0.4 mm) layer of polyethylene tape. Its main purpose is mechanical protection of the underlying coils.

The present overwrap for the switch and coil package is a coarsely woven fiberglass cloth sprayed with a contact adhesive to keep it from unraveling. This provides overall and first-level protection.

Since this coil package is in direct contact with the passing wheels, it will suffer wear and eventually fail (probably due to a break within a coil or a failure of a solder joint). With this in mind, the whole package is expendable. Replacement involves only two nuts and three electrical connectors.

The test rail section (Figs. 7 and 8) has a pocket machined into the head to hold the magnet, and a recess along the top of the head for the coil package. A tapered transition into and out of this recess helps to transfer

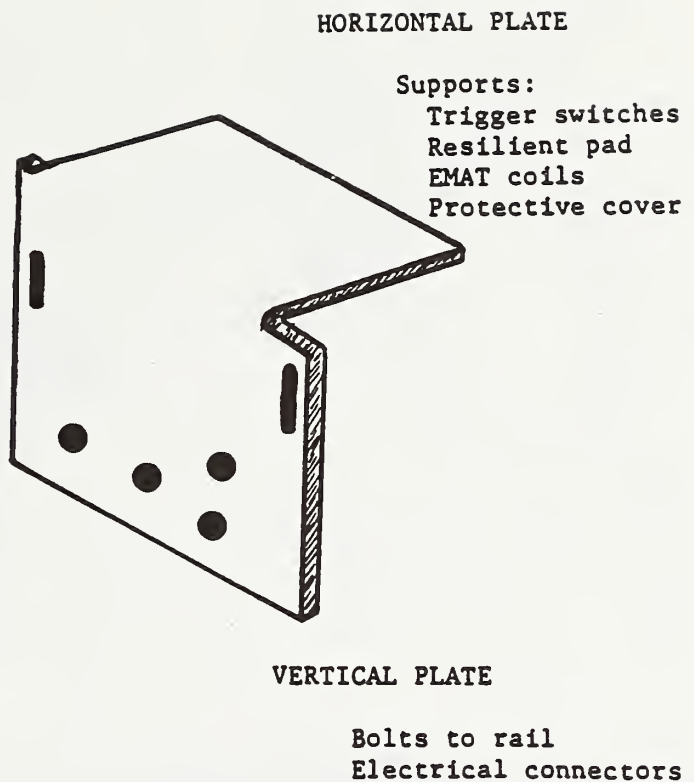


Figure 5. This aluminum bracket is the support structure for the coil package. It is bent from a 1.6 mm sheet.

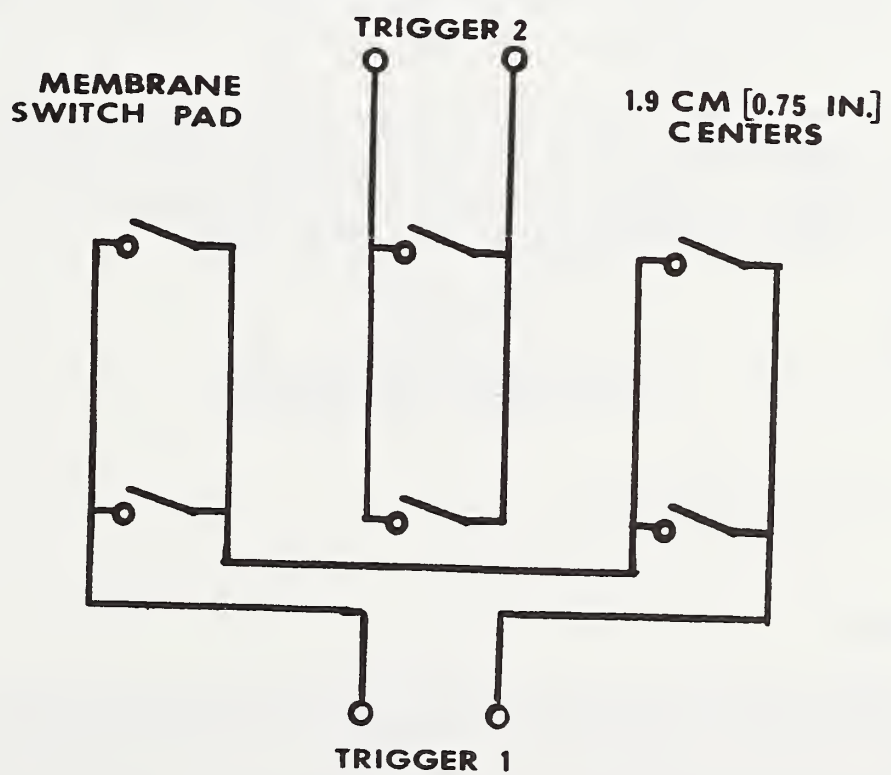


Figure 6. Membrane switch pad used as a wheel trigger. These connections give two separate triggers.

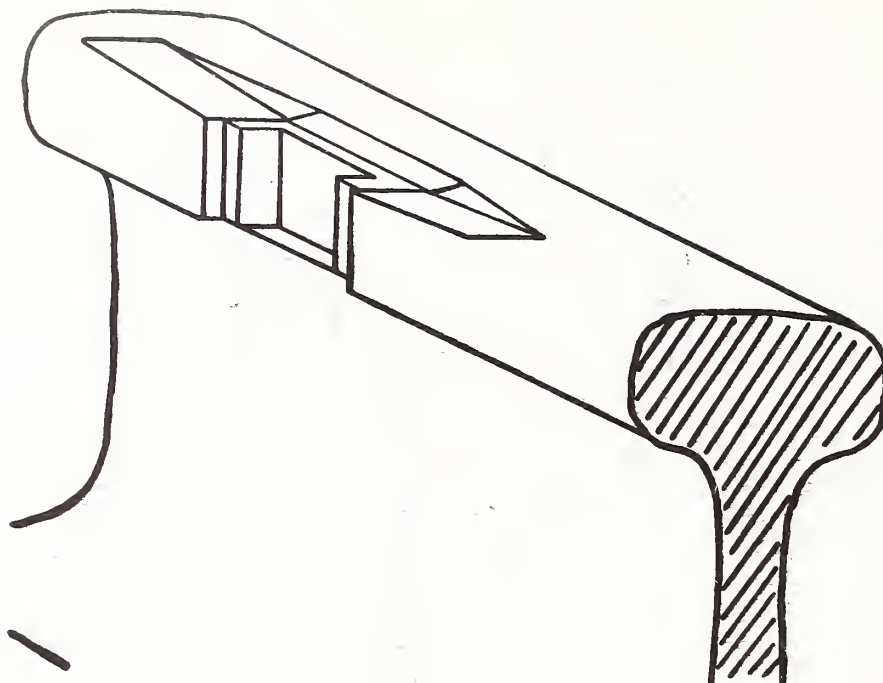


Figure 7. Schematic of the machining necessary to put the EMAT transducers in the rail. The deep pocket is for the magnet, while the tapered recess along the top is for the coil package. The rail section is 67.5 kg/m (136 lb/yd) with a length of 1.7 m (65 in).

load smoothly to the remainder of the rail head for wheels with "false flanges" and minimizes stress concentration and fatigue problems. Bolts on either end of the pocket anchor the EMAT.

Figures 9 and 10 are cross sectional views of the EMAT within the rail and indicate how the foam compresses into the recess while the remaining rail head bears the weight. Figures 11 and 12 are photos of the coil package assembly and the EMAT insertion into the test rail.

OPERATIONAL PRINCIPLES

There are four basic subsystems.

Transducer Package

The EMAT transmitter and receiver coils with their magnet are inside the recess machined into the test rail. Integral to this package is the pad of membrane switches that trigger in the presence of a wheel. The magnet inside its copper box should be permanent. The coil package mounted on an aluminum bracket is subject to wear and will need occasional replacement. The coils and switches connect by coaxial cables to the analog electronics.

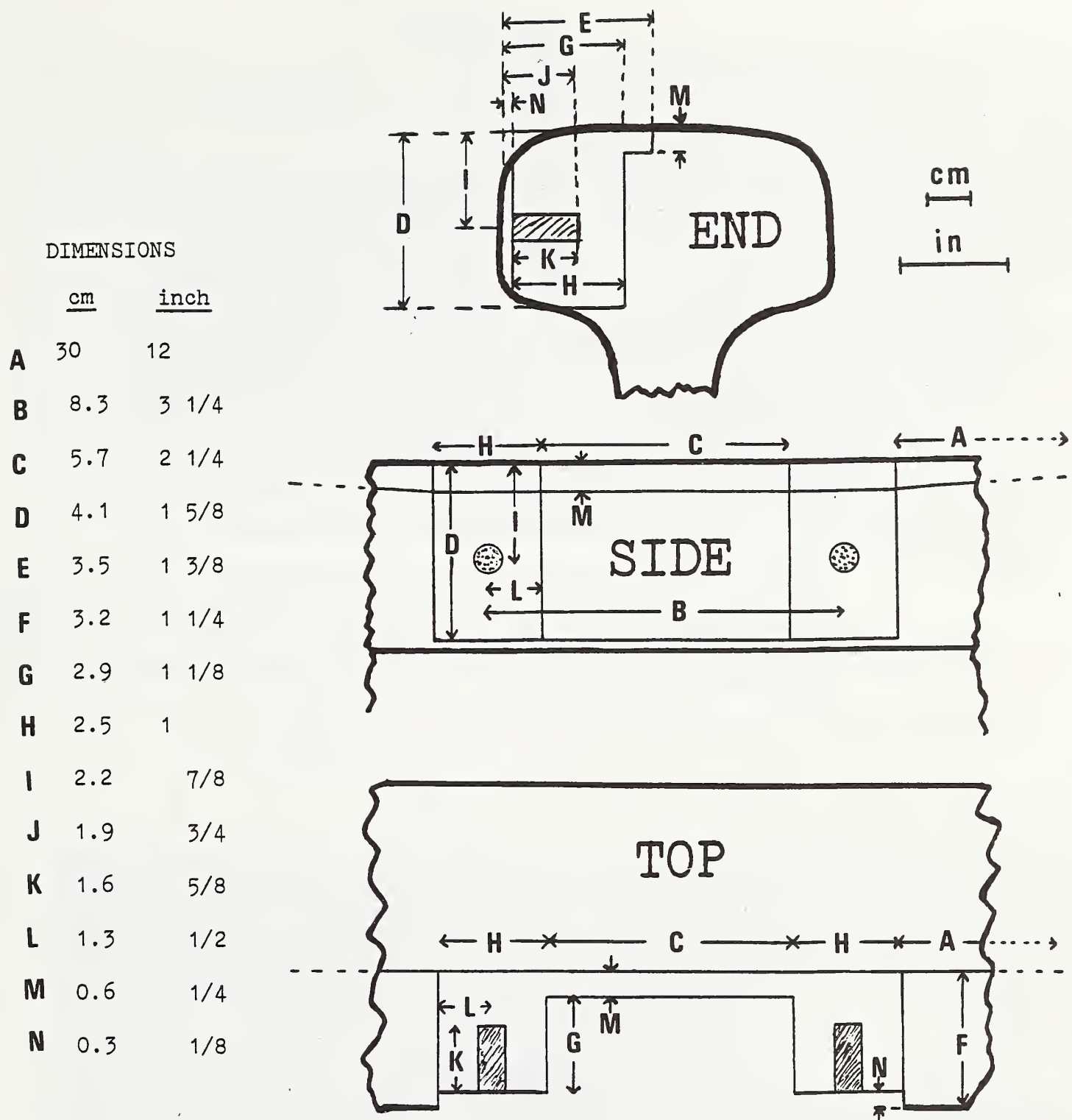


Figure 8. Dimension and details of pocket machined into test rail. The transition section extended 30 cm (12 in) on either side of the coil package. It tapered from a depth of 0.6 cm (1/4 in) at the EMAT in a straight line back to the surface of the rail head.

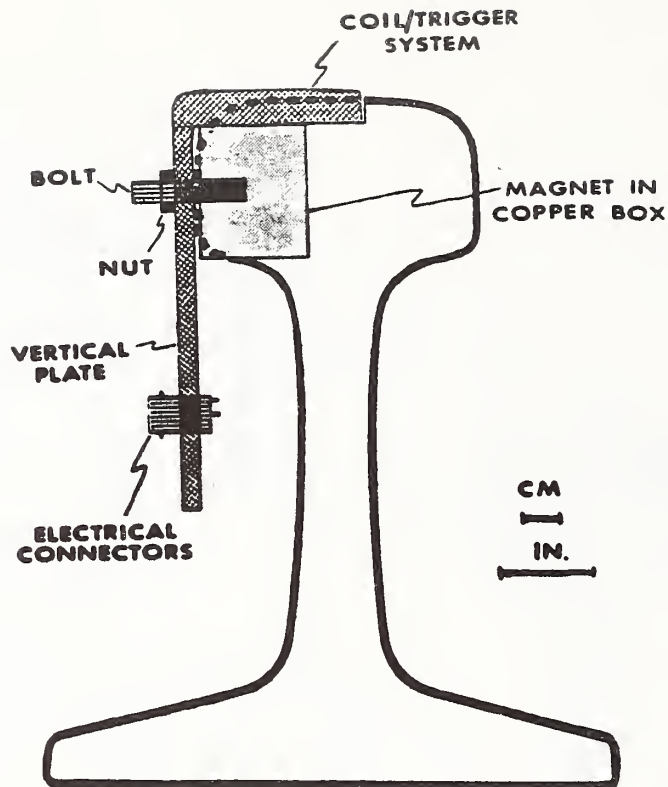


Figure 9. Cross section of EMAT system within the test rail. The distance between the vertical plate and the box is adjusted with washers to assure a 3-4 mm space between the end of the horizontal plate and the lip of the tapered recess. (See EQUIPMENT INSTALLATION.)

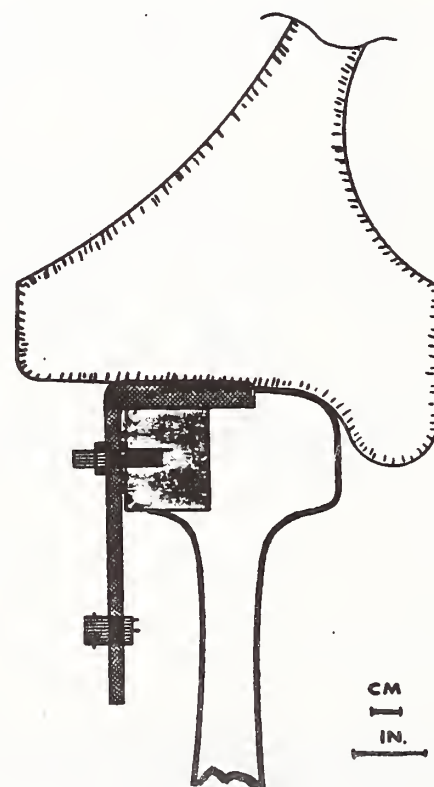
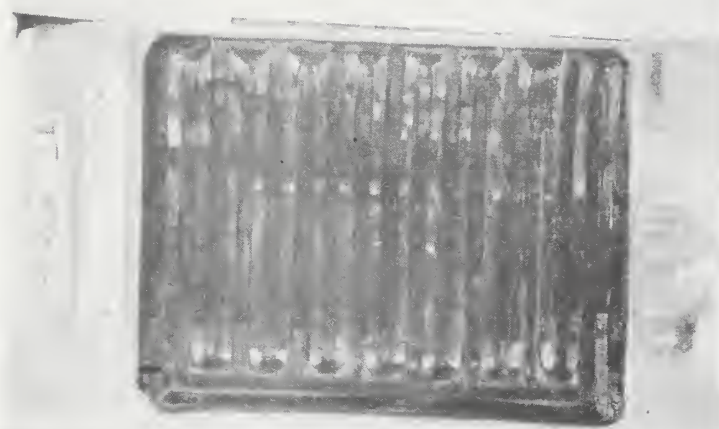
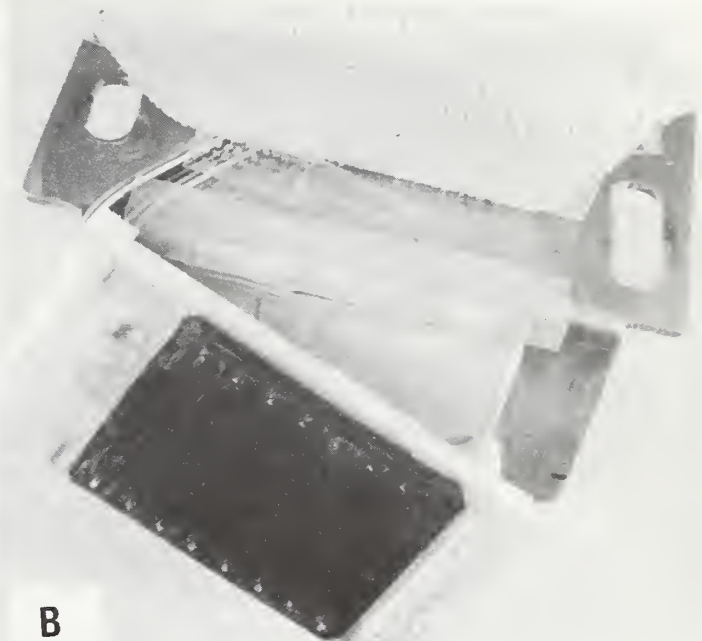


Figure 10. Cross section showing how the wheel compresses the coil package into the machined recess while the remaining head bears the weight.

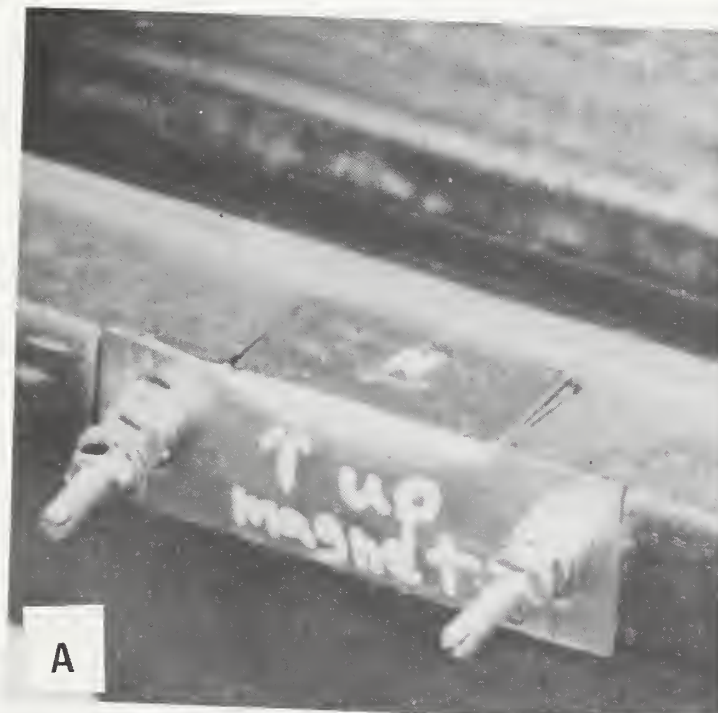


A

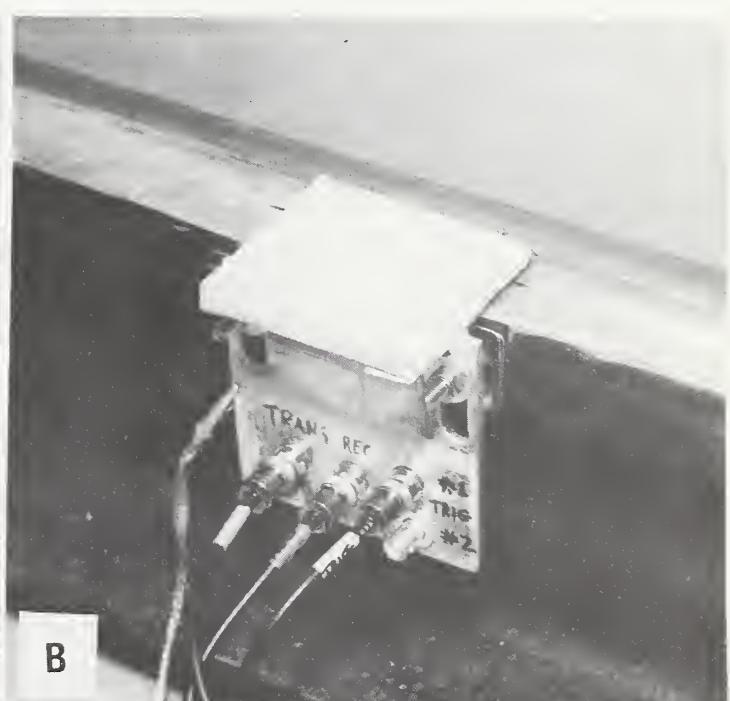


B

Figure 11. A. Detail of the two EMAT coils on their fiberglass/epoxy support.
B. Multiple layers on the horizontal plate of the coil package.



A



B

Figure 12. A. Magnet/copper box mounted on test rail.
B. Coil package in position.

Analog Electronics

There are two parts to this package:

- a. A high-current rf amplifier to produce gated pulses (10 cycles) at 500 kHz for the transmitter.
- b. A high-gain, low-noise amplifier for the receiver signal. This section also contains a detector and log amplifier.

Digital Electronics

This package processes the analog signal (the detected envelope of the rf). The front end contains integrated circuits to:

- a. Detect the peaks found in the first 2.5 ms of signal after the trigger generated by the passing wheel. This is enough time to complete the first two round trips (RTs) of the acoustic signal.
- b. Digitize the amplitude and time of every peak found.

A microprocessor then uses the software in an EPROM to analyze this peak information. Each wheel will generate one of five flags:

- a. No test. There was no recognizable signal.
- b. Poor metal. The signal was so highly attenuated that the second round trip disappeared.
- c. Critical flaw. There was a large flaw echo.
- d. Multiple flaws. There were more than three flaw echoes.
- e. Wheel OK.

Report Station

This is a small personal computer connected to the digital electronics by an RS-232 bus. This unit receives the flag signals from the microprocessor and prepares the final test report. It can be located in a location remote from the rest of the equipment.

Figure 13 is a block diagram of these four subsections, while Fig. 14 is a logic diagram of the overall process integrating the hardware and software systems.

EQUIPMENT INSTALLATION

In-Track EMAT

EMAT installation must follow a sequence.

1. Install the test rail in the track. The magnet pocket and tapered recess must be on the outside.
2. Screw in the two threaded rods (1/4-20) on either side of the magnet pocket. These are 3.8-4.4 cm (1 1/2-1 3/4 in) long and will seat firmly in the drilled and tapped holes with about 2.5 cm (1 in) protruding. They do not have heads, but there is a

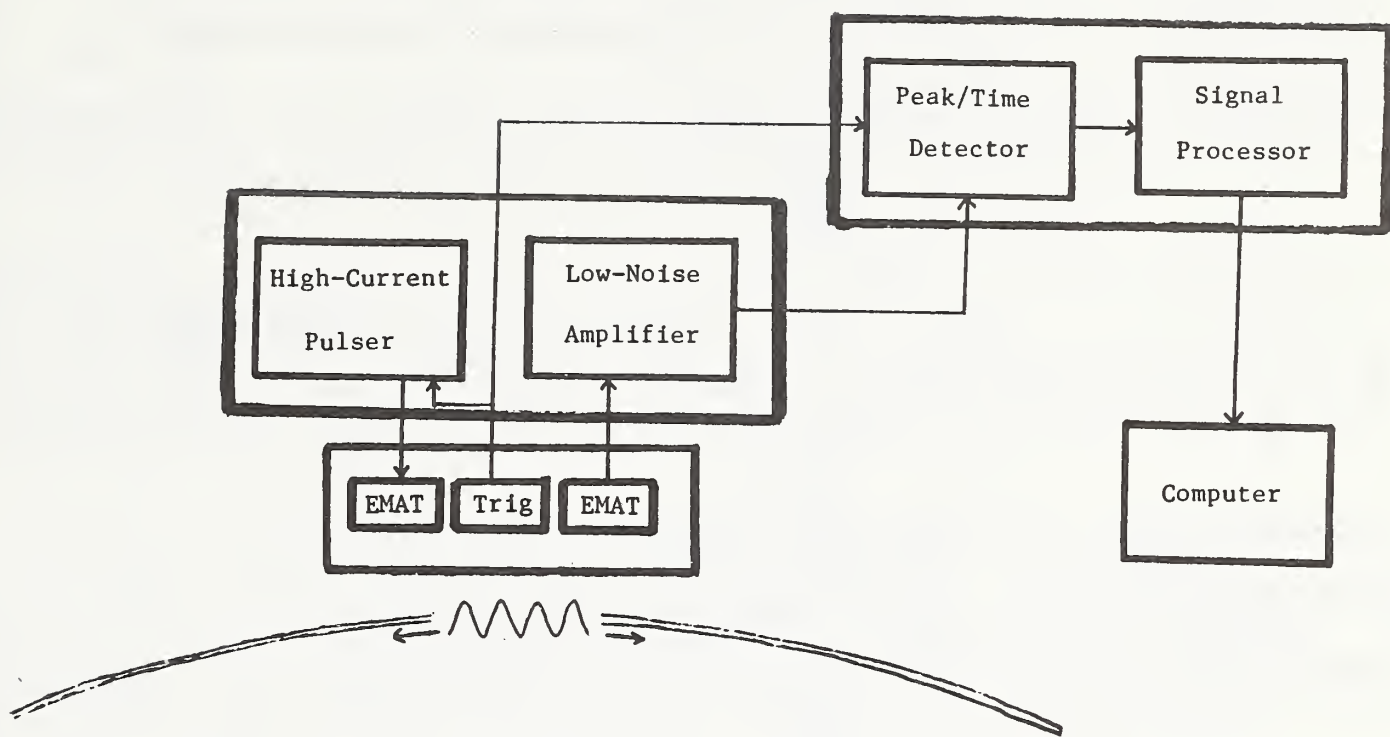
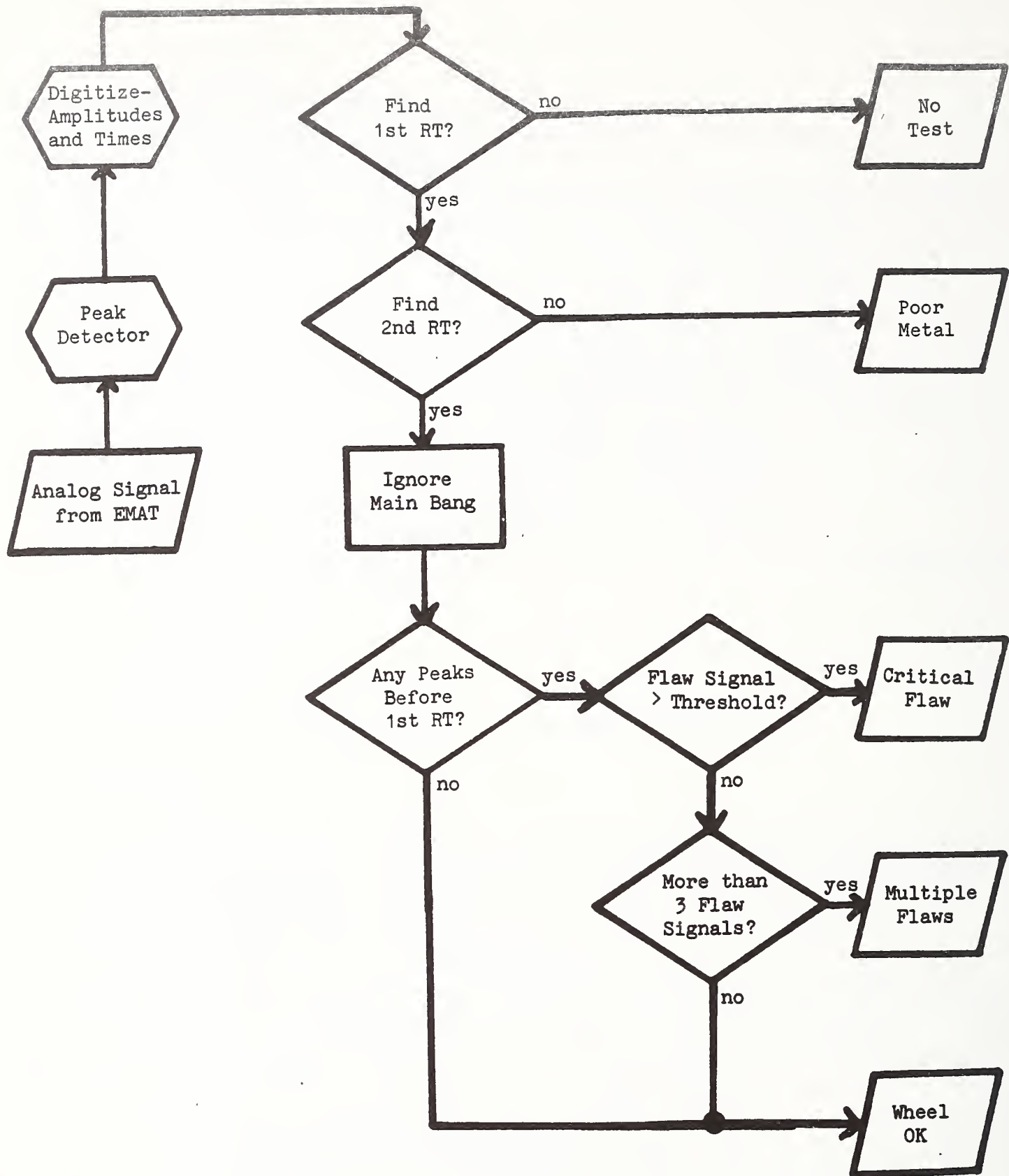


Figure 13. Block diagram showing the relationship of the in-rail transducer package, the analog electronics, the digital electronics, and the reporting computer.

screwdriver slot in the end. To allow subsequent removal, it is best to grease the threads.

3. Insert the magnet into its copper box. The magnet must be oriented so that its field is directed into the passing wheel (perpendicular to the top of the rail head); north or south pole must point directly up. The magnet is very strong and will jump at any ferromagnetic material (e.g., the rail), and will pull itself into the rail pocket. Use great caution to hold the magnet firmly and avoid crushing fingers between rail and magnet. Ease the box into its location; the two bolts should pass through the slots in the box wings. A cautiously used screwdriver in the pocket and behind the box may help maintain control.
4. Place a washer and nut on each bolt and tighten.
5. Determine the number of washers on each bolt that will provide the proper spacing of the coil package from the outside edge of the rail head. The horizontal plate (Fig. 5) has a cover to protect the various components. To minimize cutting this cover, the far edge (on the inside of the track) should be about 3-4 mm from the edge of the tapered recess (Fig. 9). As the foam collapses under the wheel weight, the cover folds into this space. Stack enough washers (atop the nut holding the magnet in place) to maintain this distance when the coil package is in place.



Hardware

Software

Flags

Figure 14. Logic diagram to show the operation of the systems shown in Fig. 13. (RT = acoustic round trip signal.)

6. Position the coil package in the tapered recess. The slots in the vertical plate will pass over the bolts and rest on the stack of spacer washers. Tighten a locking washer and nut on each bolt.

When replacing a coil package, remove only the outer nut and locking washer on the two bolts. Remove the old package, position the new one, and replace the washers and nuts.

Connections and Cables

Figure 15 shows the interconnections between the four subsystems. All the cables are coaxial type with BNC connectors except for the RS-232 link to the reporting computer.

The cable connecting the in-rail package ("track cable") is special because of its length (10 m), and its shield of metal braid. While this braid does bind the three coax cables together and helps to protect them from mechanical damage, its main function is electrical shielding to minimize noise pickup. For this reason, on each end there are alligator clips that should be attached to the frames of the coil package and the analog electronics.

While the individual lines within the track cable are identified, there is very little or no difference in the signal if the transmitter and receiver connections are exchanged. For the sake of consistency, though, it is probably better to follow the ID markings.

The length and type of the track cable are important. Both transmitter and receiver circuits have been tuned with this cable (10 m of RG-58C/U) to account for its capacitance. A different length of cable will require adjustments to this tuning. (See the ELECTRONIC SCHEMATICS section.)

The two cables between the analog and digital electronics can be any convenient length and type. Within the specifications of the standard, the same is true of the RS-232 cable going to the output computer.

On the reporting computer, there are special cables between CPU and monitor, and also between CPU and keyboard. A printer is required only if a hard-copy report is desired after a train passes.

The digital oscilloscope in Fig. 15 is not necessary. It is merely a means of visually monitoring the signals as they are generated. The trigger and acoustic signal can be teed off either analog or digital electronics.

Although not indicated in Fig. 15, each of these electronic boxes requires its own connection to a standard 110 V, 60 Hz power source. The computer has its own separate plugs for the CPU and the monitor.

Report
Station

Digital
Electronics

Analog
Electronics

Transducer
Package
(in-rail)

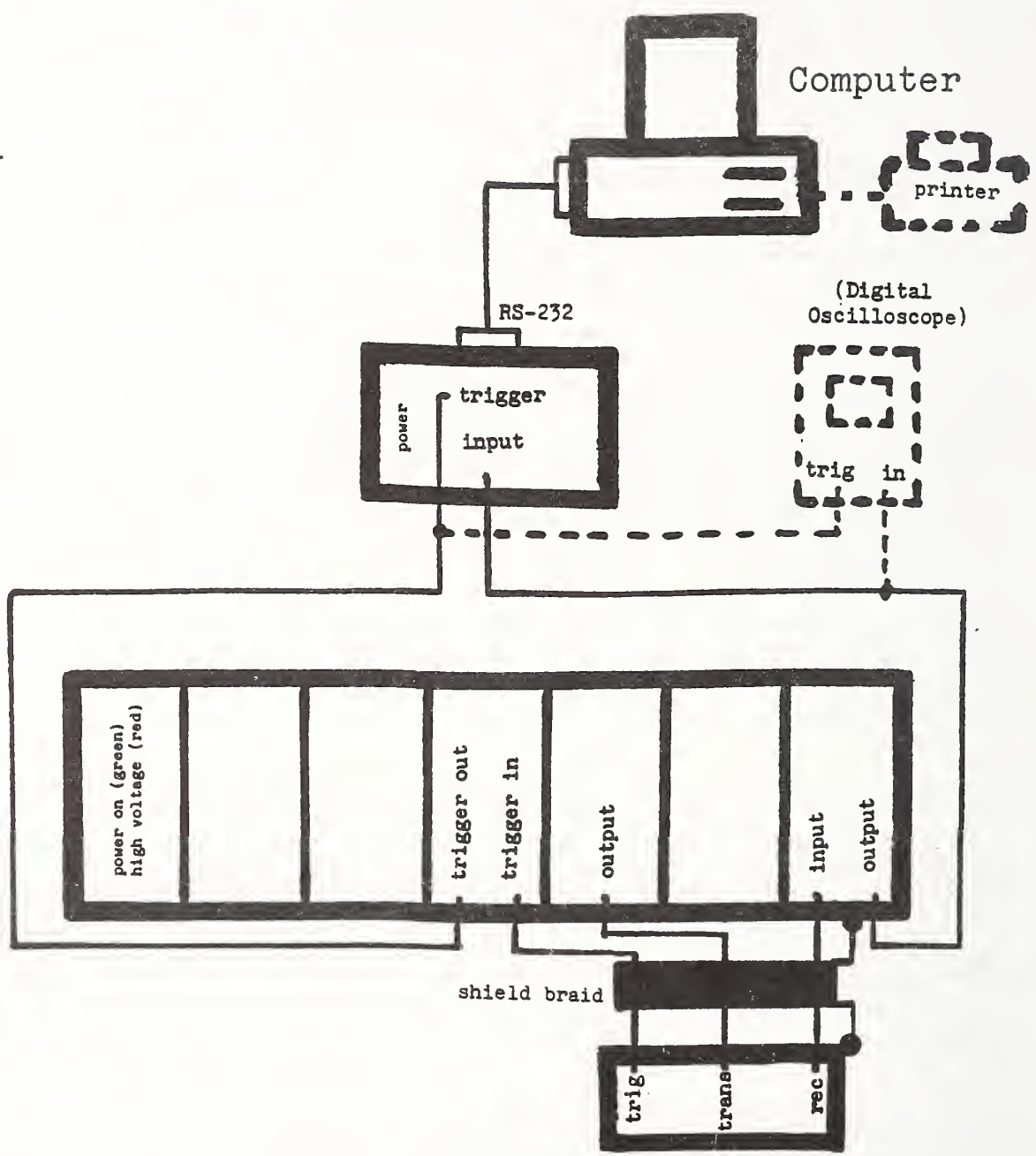


Figure 15. Diagram of cable connections between the four subsystems. The track cable is shielded by a metal braid. The digital oscilloscope is only a monitor and not required for operation. The printer is required only if a hard-copy report is desired.

EXPERIMENTAL RESULTS

Initial development of EMAT design and electronic equipment was done in a static mode. Later, to simulate dynamic operations, we established a standard gauge test track in our laboratory that was 2 m long (Fig. 16). TTC provided us with several wheel sets (two wheels on an axle) that we could roll back and forth over our sensor. Subsequently, we had the opportunity to conduct field tests at TTC (Fig. 17).

Laboratory Tests

The major items to test on the in-track unit were:

1. Geometry.
 - a. The depth of the track recess necessary for the coil package.
 - b. The lateral location of the EMAT coils.
 - c. The effect of the lateral position of the wheel.
 - d. The depth of the foam necessary to accommodate the taper on the wheel tread.
 - e. A preliminary look at the effect of variations in the tread wear profile.
2. Trigger operation.
 - a. Pressure required to operate the membrane switches reliably.
 - b. Effect of the direction of wheel travel.
 - c. Repeatability.
3. Response to variation in the small range of velocities possible.

Of course, having a consistent and realistic source of acoustic signals was necessary to understand how to interpret the information available. This has to precede the development of any analysis software.

Acoustic Signatures

The oscilloscope traces in Fig. 18 are indicative of a few types of acoustic signals recorded in the laboratory. All these waveforms are after electronic detection and log amplification. The data are from 0.91 m (36 inch) diameter wheels.

Wheel OK

The wheel in Fig. 18A had been taken from service, but the tread was recently machined to restore the profile. This wheel was in good condition and the signal shows no flaw indications. Note the excellent signal/noise ratio that give a very clean baseline and makes any acoustic signals very prominent.

The large spike at zero time is due to the gated rf pulse in the transmitter coil inducing a pulse in the receiver coil which overloads its amplifier. This is frequently identified as the "main bang." During this recovery time, we are unable to see an acoustic echo. This signal merely indicates that the system is operating.

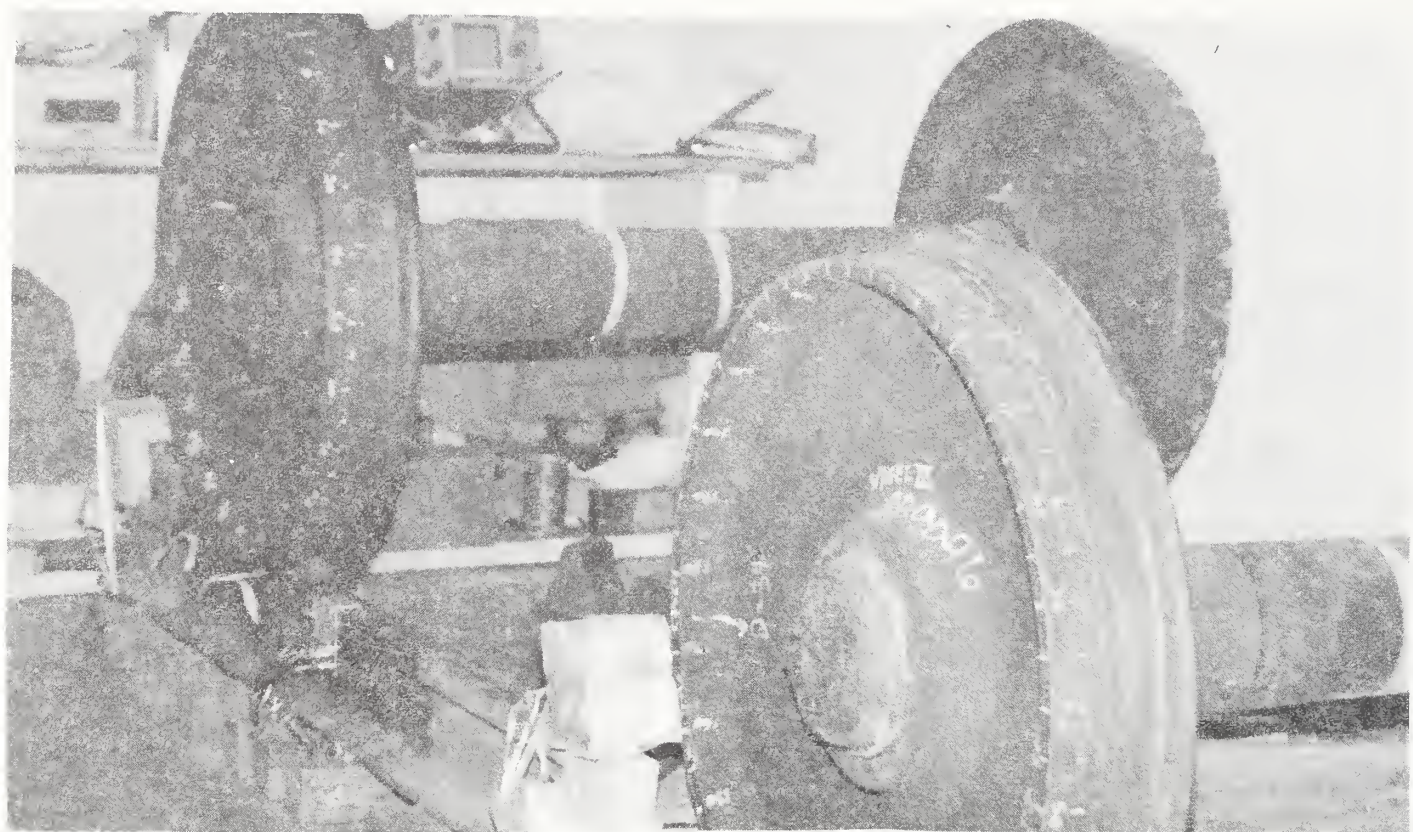


Figure 16. Full scale test track established in our laboratory. Wheel sets rolled over the EMAT. Total length was about 2 m.



Figure 17. Test site established on the Impact Track of the Transportation Test Center in Pueblo, Colorado. The electronics were housed in the trailer.

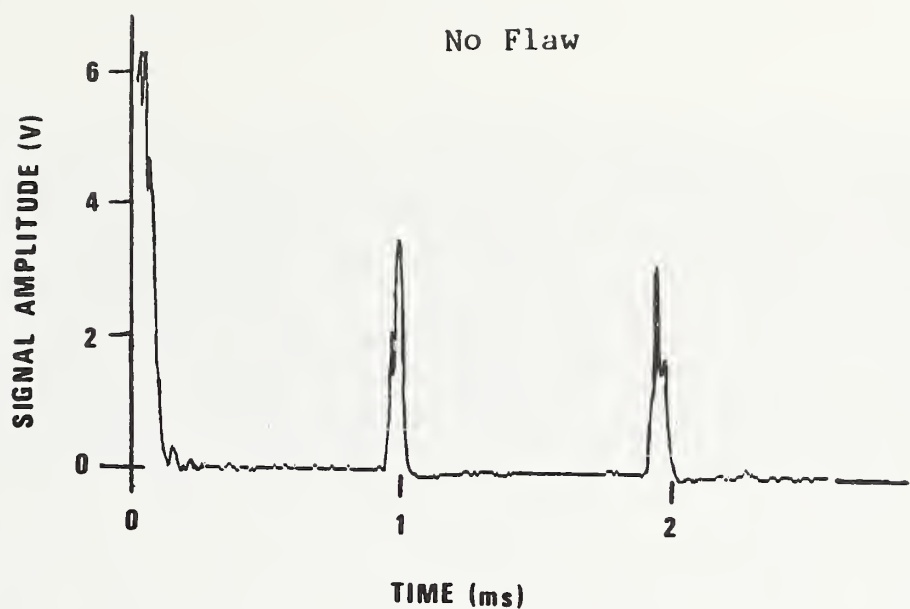
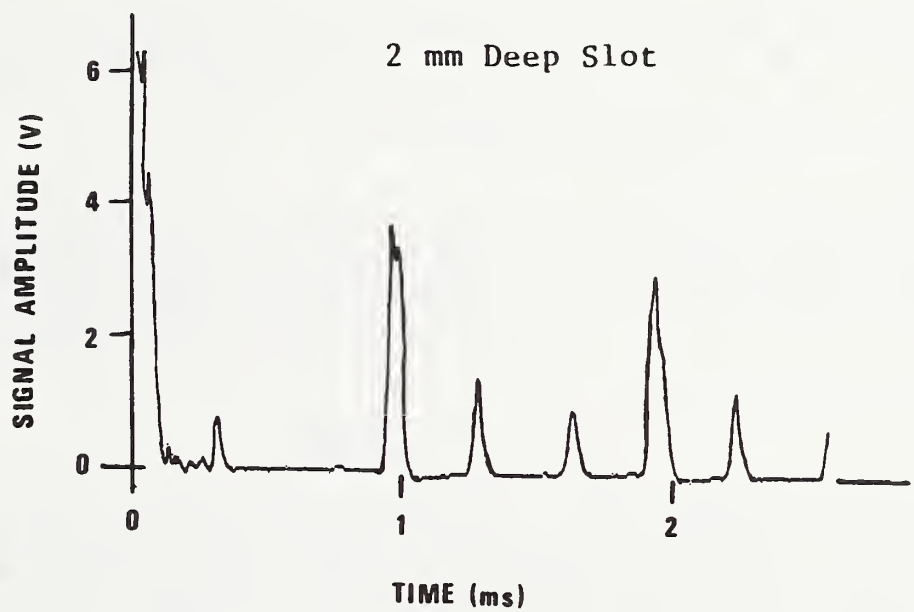
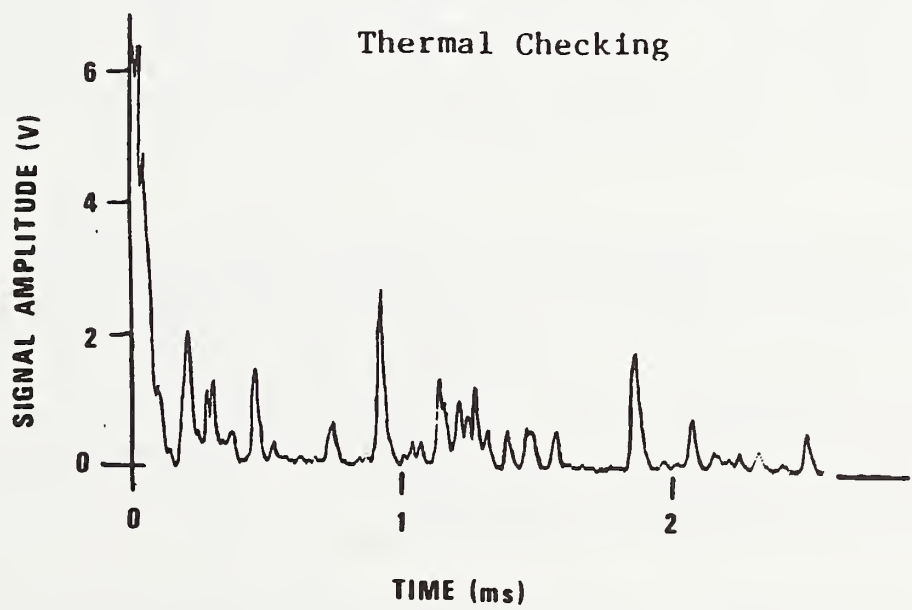
A**B****C**

Figure 18.

Typical analog signals. A and B are from the same wheel before and after cutting an artificial flaw. The wheel in C had been condemned for thermal checking and removed from service.

The signals occurring at approximately 1 and 2 ms are the first and second round trips (RTs). Depending on the metallographic condition of the wheel, the acoustic pulse can travel many times around the wheel (we have seen as many as 18), or very few. In the signal analysis, the arrival time of the first RT is indicative of the wheel size. If this signal is not seen, no test is possible and the digital system raises a flag (Fig. 14). All materials normally attenuate the signal amplitude, so each successive round trip is smaller. If the microprocessor cannot find the second RT signal, it raises a flag that the metal may be in very poor condition.

Single Flaw

The data in Fig. 18B are from the same wheel used in Fig. 18A, only now we have machined a semicircular slot (2 mm deep and 12 mm long at the surface) into the center of the tread. The additional signals are echoes from this artificial flaw. There are multiple returns because there are multiple acoustic paths for the signal to travel.

Our current algorithm looks for peaks between the "main bang" and the first RT. If the flaw signal amplitude exceeds 20% of the first RT amplitude, it raises a critical flaw flag. This 20% figure is based on very limited laboratory experience, and experience will undoubtedly dictate later adjustments.

Multiple Flaws

Figure 18C shows the signal from a wheel condemned for thermal checking. The likelihood of a single deep crack is small, since whatever causes one crack will probably cause many more around the tread. If more than three peaks appear between the "main bang" and the first RT, the analysis raises the multiple flaws flag. Because of the high signal/noise ratio (Fig. 16A), we have confidence that each peak here is a true indicator of a flaw.

Blind Spots

The signal in Fig. 18A shows no echo returns from any flaws. The unavoidable presence, however, of the "main bang" would mask any indication of flaws near the transducer--the signal would simply be lost. The same problem exists for any flaws exactly opposite the transducer; their echo would be lost in the round trip. This means that a short section of the tread at the top and bottom of the wheel (as it triggers the ultrasonic pulse) will not be inspected. We estimate that these two hidden areas amount to about 20% of the circumference.

In practice, this ability to see only about 80% of the tread may not prove to be much of a problem. Our limited experience has indicated that real flaws usually occur in large multiples. If this observation holds up in field use, the hidden area will contain only a small number of the flaws present. The analytical algorithm will likely raise a flag on the basis of the remaining flaws detected. Of course, it is always possible to use two sensors with a spacing of about a quarter of a wheel circumference.

Field Tests

Of course, no amount of laboratory work could substitute for actual tests on a rail line. TTC provided us this essential opportunity on three separate occasions. They installed our test rail on their Impact Track and established a trailer to house the electronics so we could run week-long tests on November 13-17, 1989, and May 14-18, 1990. On June 25, 1990, we left the equipment on site for TTC personnel to operate until July 12. The tests began with simply rolling wheel sets (as we did in the lab) to establish initial setup, and graduated to running an engine and several consists (Fig. 17). The rail cars were empty in some cases and 20% overloaded in others. The wheels ranged from brand new to condemned from revenue service.

Included among the things learned and the things modified as a result of this experience:

1. There were two design changes in the aluminum bracket support of the coil package. While this unit does not bear the weight of the passing train, it does see enough load that the thickness must be sufficient to avoid deformation. One wheel with a heavily worn profile had so much overhang below the top of the rail head that we had to remove a projection of the horizontal plate that extended past the vertical plate.
2. Even though the rail flexed quite noticeably as each wheel passed, the magnet in its copper box did have sufficient space that it was not crushed or deformed.
3. As determined by TTC engineers, the modified rail section was sufficient to support fully loaded cars, 143 000 kg (315 000 lbs) on eight wheels.
4. To obtain some degree of reliability in the trigger system, we advanced from a single membrane switch to the pad in Fig. 7.
5. On occasion, it was necessary to insert a 2-4 mm thick spacer between the magnet box and the coil package. This raised the top surface and generated more pressure through the foam pad to close the membrane switches.
6. Some software changes improved the communication between the digital electronics and the reporting computer.
7. Hardware changes in the digital electronics increased the time resolution of the peak detector.
8. The high-current traction motors of the locomotive did often generate noise in the baseline of the acoustic signal when they were directly over the EMAT. However, even for the first wheel after the locomotive, there was no indication of noise from this source. The coils appear to be well shielded by the rail and the wheel under inspection.
9. All the electronics functioned properly with power from a portable 10 kW generator.
10. While one coil was cut by a wheel sliver, the major weakness in the coil package appears to be in the fatigue life of the electrical connections

11. With the redesigned switch pad (Fig. 6), the trigger system appeared reliable up to about 24 km/h (15 mph). At higher speeds (32 km/h or 20 mph), some wheels did not trigger the system - particularly, the second wheel on a truck. While such a speed does not represent a significant restriction in a rail yard, this limit is likely due, not to the switch, but to the mechanical relaxation time of the foam pad above the switches. At the higher speeds, this material does not have time to recover to its original shape before the next wheel arrives. Should this become a problem, some other foam would likely be preferable.
12. A guide rail was installed but its spacing had no effect.

Figure 19 demonstrates some specific examples of the data collected during the first test in May. The train speed here was 8 km/h (5 mph), but the appearance of the signal remained unchanged up to at least 24 km/h (15 mph). The wheel in Fig. 19A was in normal service and had no known defects. The wheels in Fig. 19B and C had been condemned and removed from use.

The signal baseline for a number of wheels with no defects was as flat as in Fig. 18A, but Fig. 19A shows considerably more structure. This may indicate the kind of threshold it will be necessary to specify in the analysis software.

The "scrape or gouge" signal in Fig. 19B shows strong echoes indicative of a single large flaw (cf. Fig. 18B). The "thermal cracks" signal in Fig. 19C is similar to Fig. 18C in having a large number of significant peaks. Some wheels with similar condemnation codes so attenuated the signal that the round trip indicators were not detectable; in this case, the program would raise the "no test" flag. The FRA report "Field Testing of Wayside Crack Detection System" by Robert K. Larson, Jr. of TTC (Feb. 1991) contains signal traces from many of the wheels tested.

ELECTRONIC SCHEMATICS

The special electronics designed and built for this project are currently in two distinct packages.

Analog

The analog electronics make it possible for the EMATs to generate and detect the ultrasonic signal. These two functions are physically separate and distinct, but the circuits are mounted in one chassis with seven modules.

Pulser: Generates a gated (generally 10 cycles, but adjustable) pulse of high current at 500 kHz when the in-track trigger closes to signal the presence of a wheel at the test station. This system also passes on a trigger to start the signal processing in the digital electronics section (see below). A series capacitor at the final output tunes the transmitter cable-EMAT system to achieve the maximum power transfer (Fig. 20A). The first five modules of the analog chassis house

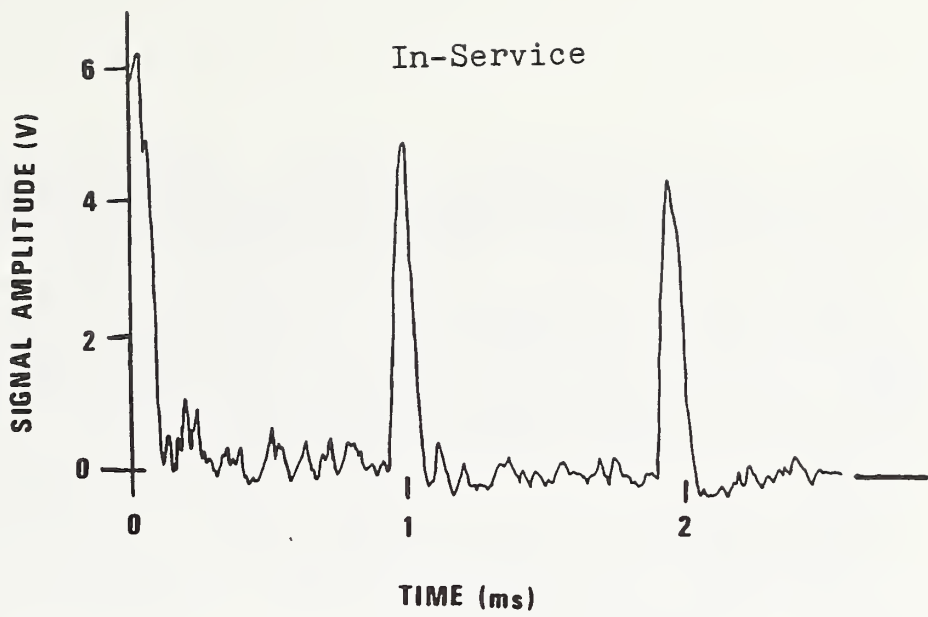
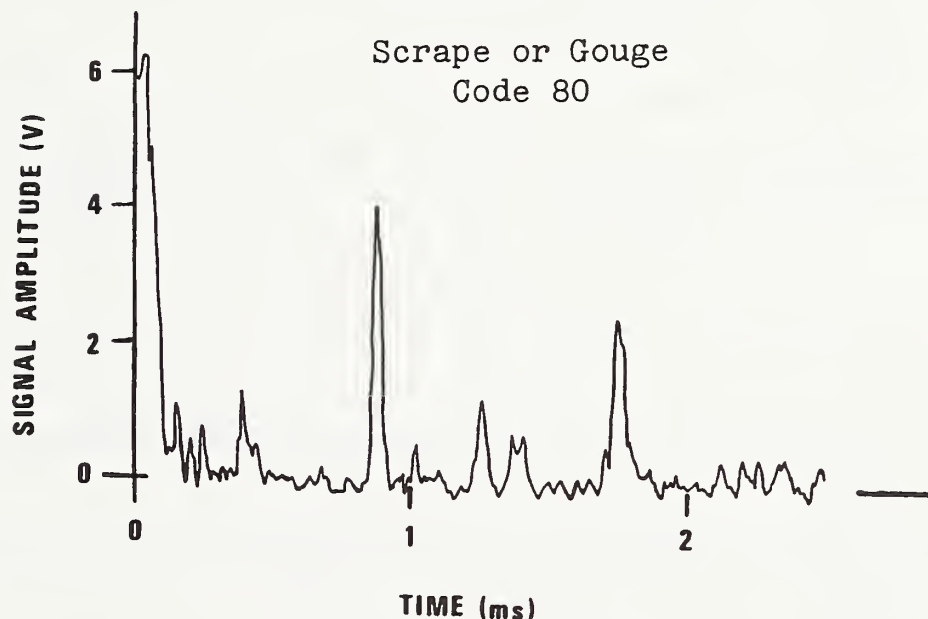
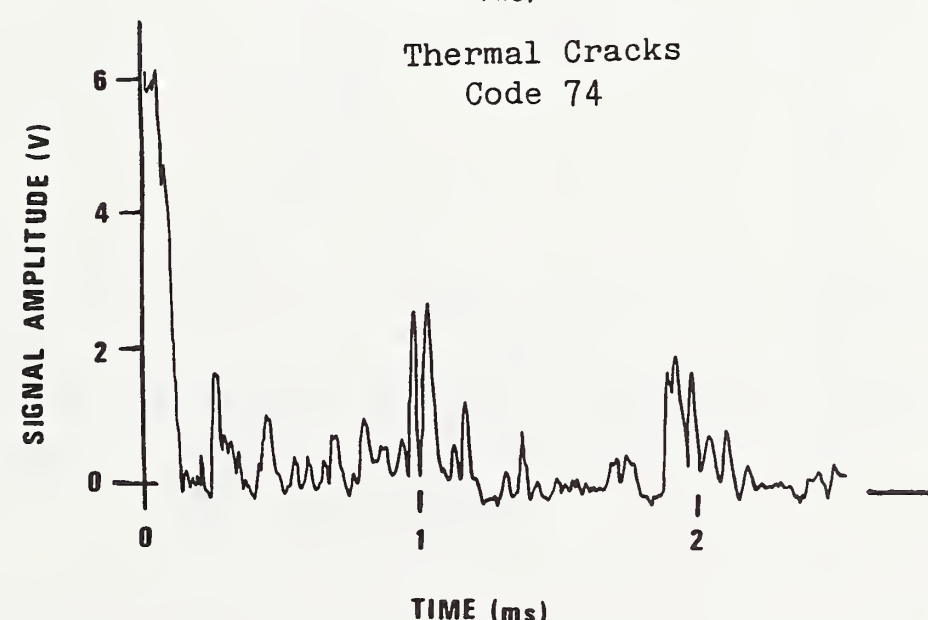
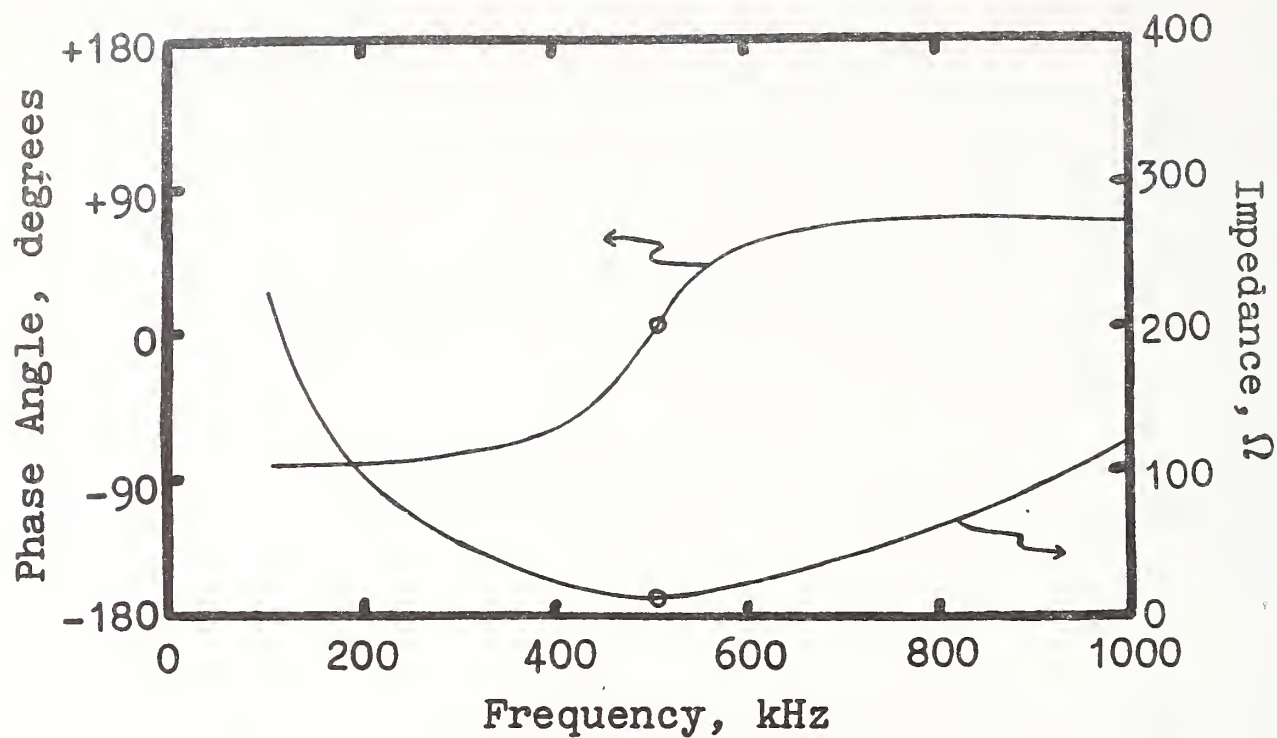
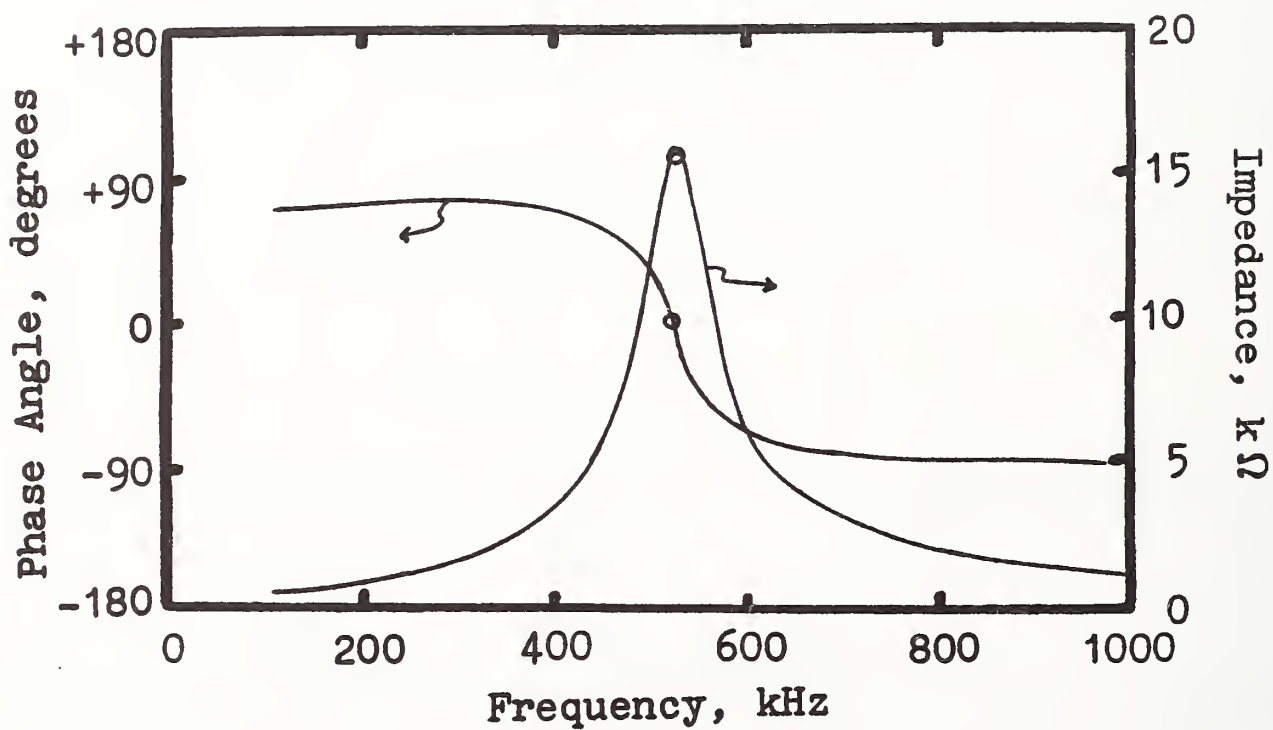
A**B****C**

Figure 19. Typical analog signals from the first field test. The wheel in A was in normal service with no known defects. The wheels in B and C were condemned and removed from use. The type of flaw and the AAR Why Made Code is indicated. Train speed was 8 km/h (5 mph).

A**B****Figure 20.**

Frequency dependence of impedance (Z) and phase (θ). The EMAT is mounted in the rail and a wheel is located on top of it. A tuning capacitor adjusted the resonant frequency of the EMAT-track cable system to approximately 500 kHz.

A. Transmitter, series-tuned for minimum impedance.

B. Receiver, shunt-tuned for maximum impedance.

this function. Figure 21 shows both the voltage and current characteristics of the transmitter pulse.

Preamp: Provides amplification with a very low noise but high (variable) gain (Fig. 22). The output delivered to the digital electronics is a detected, logarithmically amplified signal (see Figs. 18 and 19, A-C). A shunt capacitor at the input tunes the receiver cable-EMAT system to minimize signal loss (Fig. 20B). The seventh module of the analog chassis houses this unit.

Figure 23 is a schematic of the modules in the analog chassis, giving their location and connections. The module numbers run from left to right looking at the front of the chassis. Module six is empty. Figure 24 is a system photograph.

Module 1 has the electrical control switches on the front panel. The on and off sequences must always be:

ON	1. Power	OFF	1. High Voltage
	2. High Voltage		2. Power

Note: the high voltage is the last on and first off.

Among other logic operations, module 4 determines the number of rf cycles generated in each power pulse to the transmitter. This is controllable from 1-10 cycles by a thumbwheel switch on the front panel. We have normally operated with 10 cycles (setting = 0).

The gain of the preamplifier in module 7 is variable over a wide range with a ten-turn pot on its front panel. We have generally used the mid-scale setting of 400.

Figure 25 indicates the power and signal connections between circuits, Figs. 26-31.

Digital

The digital electronics process the signal generated by the analog system. Again, there are two parts (on the same printed circuit board).

Peak detector: Extracts amplitude and time information of each peak above a noise cut-off. The inputs are the preamp signal and the pulser trigger.

Microprocessor: Uses the software in an EPROM to analyze these peaks and determine whether a flaw is present. This decision goes to the reporting computer.

In Fig. 24, the digital system is in the box sitting on top of the analog chassis. Figures 32-33 are the schematics of each of the circuits.

List of Electronic Components

The following list identifies the components of both analog and digital electronics (Figs. 24-34).

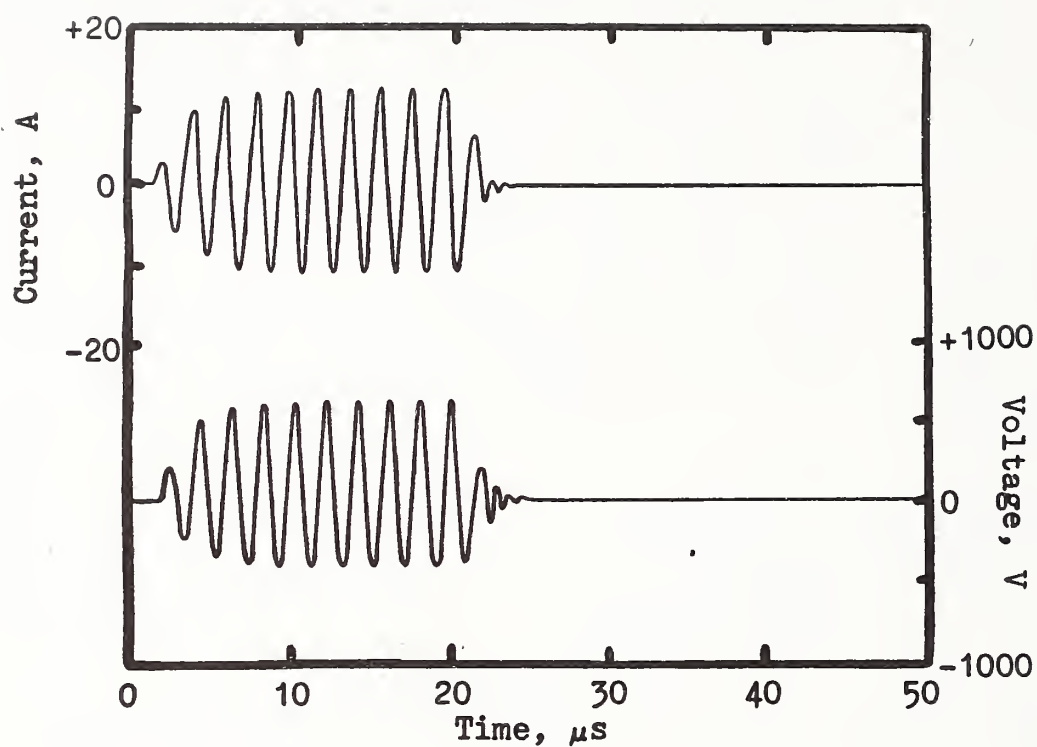


Figure 21. Voltage and current characteristics of the gated pulse delivered to the transmitter EMAT.

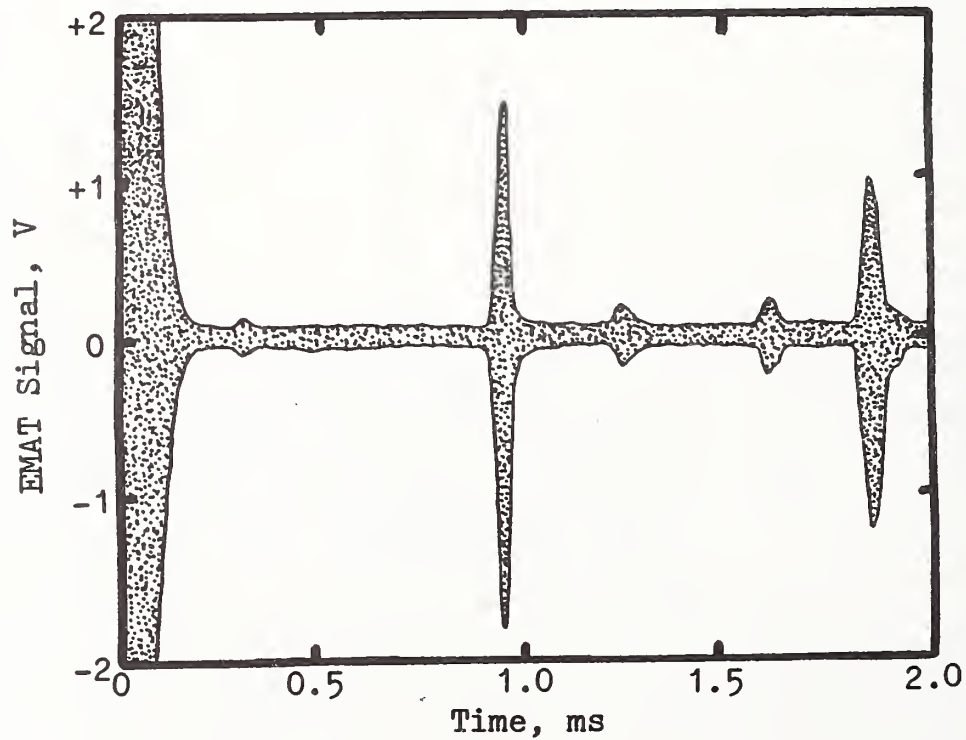


Figure 22. Sample of the receiver EMAT rf signal from the pre-amp. Figure 18 is after detection and log-amplification. Expansion of the time scale would make it possible to see the individual cycles. Subsequent round trip and echo signals repeat until they are finally attenuated into the noise.

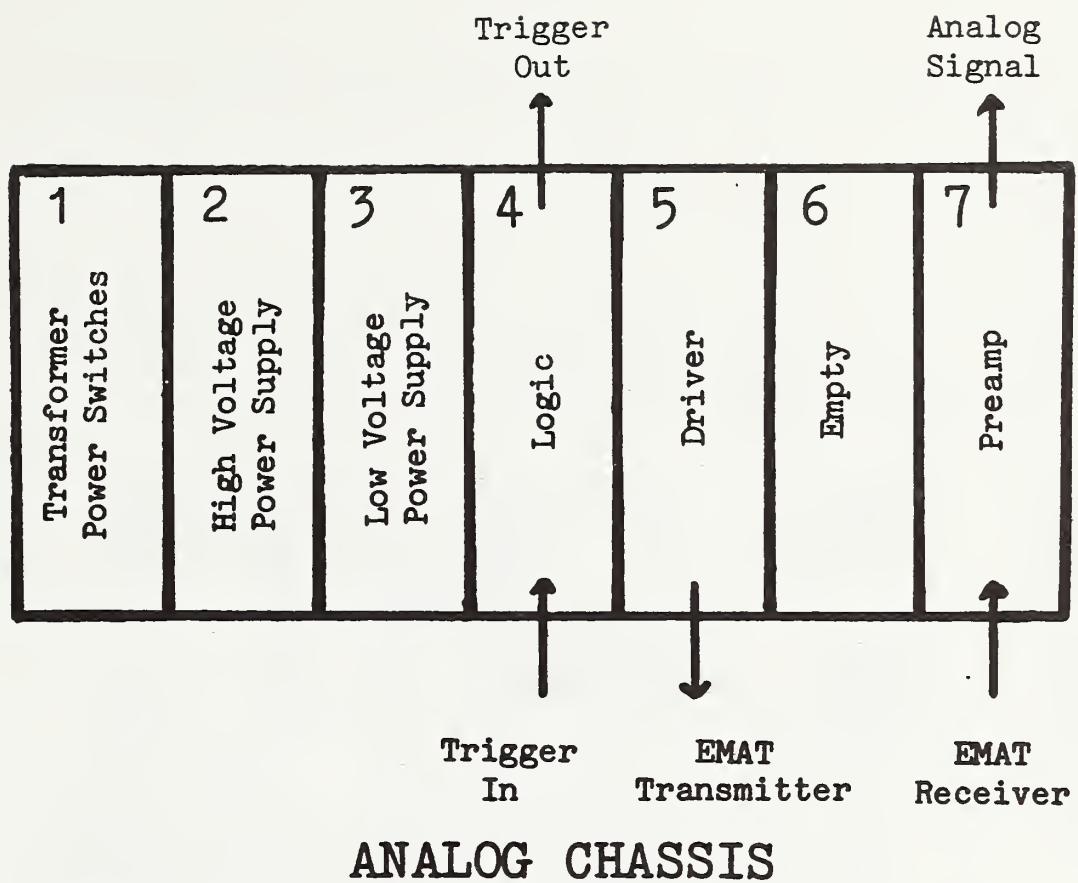


Figure 23. Schematic of the analog electronics chassis. This identifies each of the modules, its location, and connections. (Front view.)

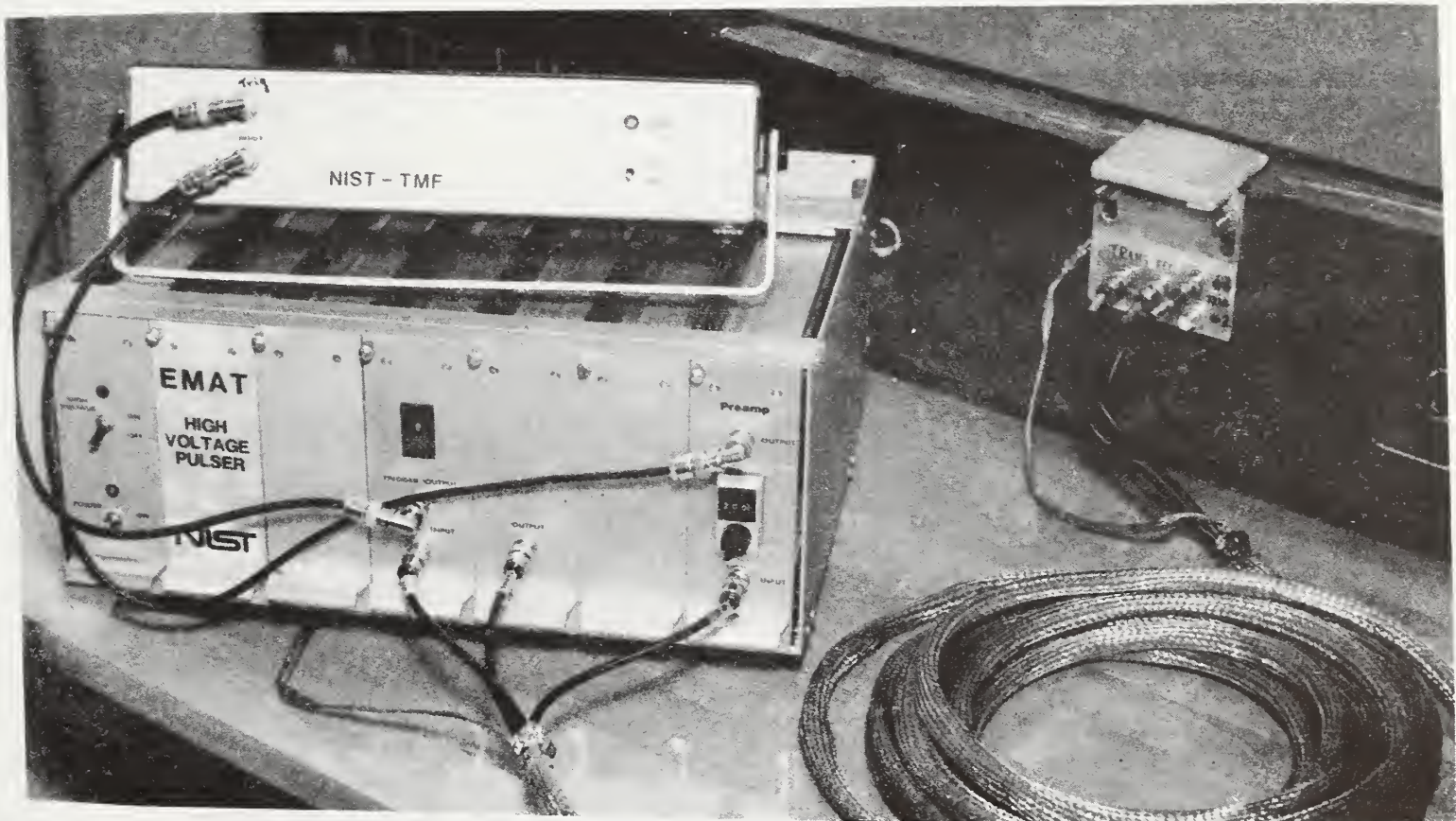
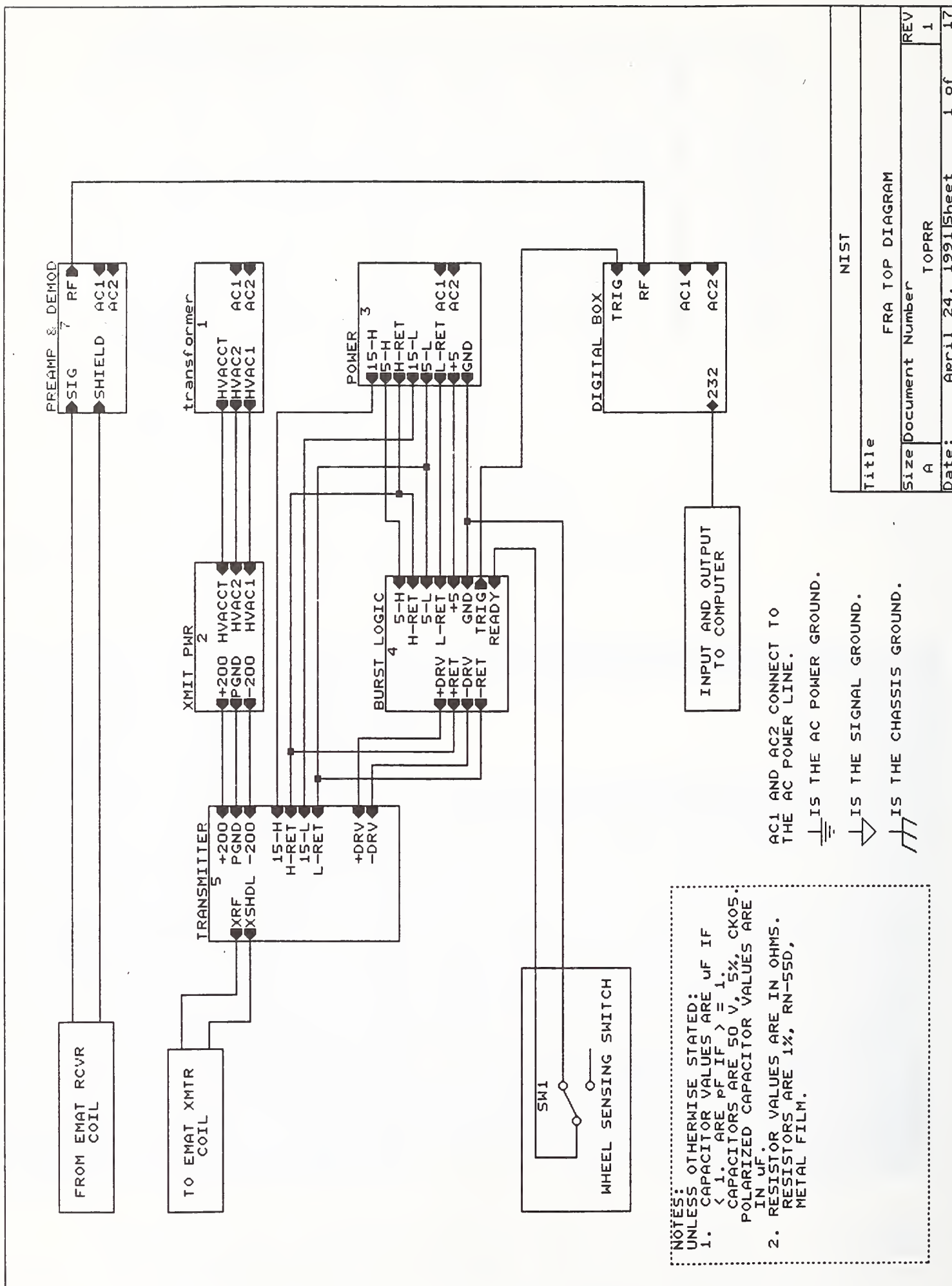
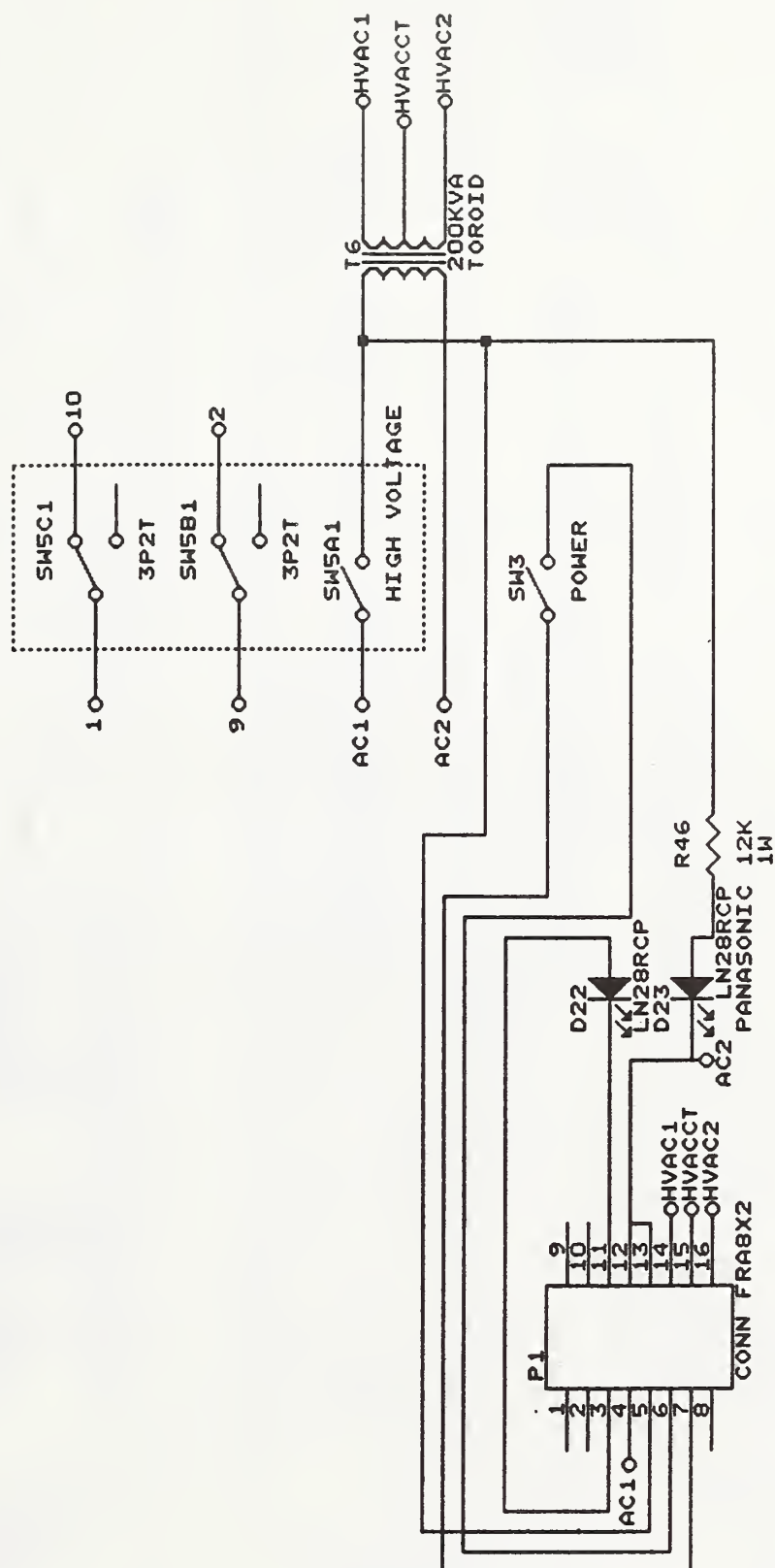


Figure 24. Photograph of all the special made parts of the crack detection system: (1) analog chassis with seven modules, (2) digital unit sitting on top, (3) 10 m cable, and (4) EMAT inside the test rail.





NIST		
Title		FRA MODULE 1
Size	Document Number	HVXFMR.FRA
A		REV 1
	Date: April 24, 1991 Sheet 6 of 17	

Figure 26. Transformer and power switches in module 1, analog box.

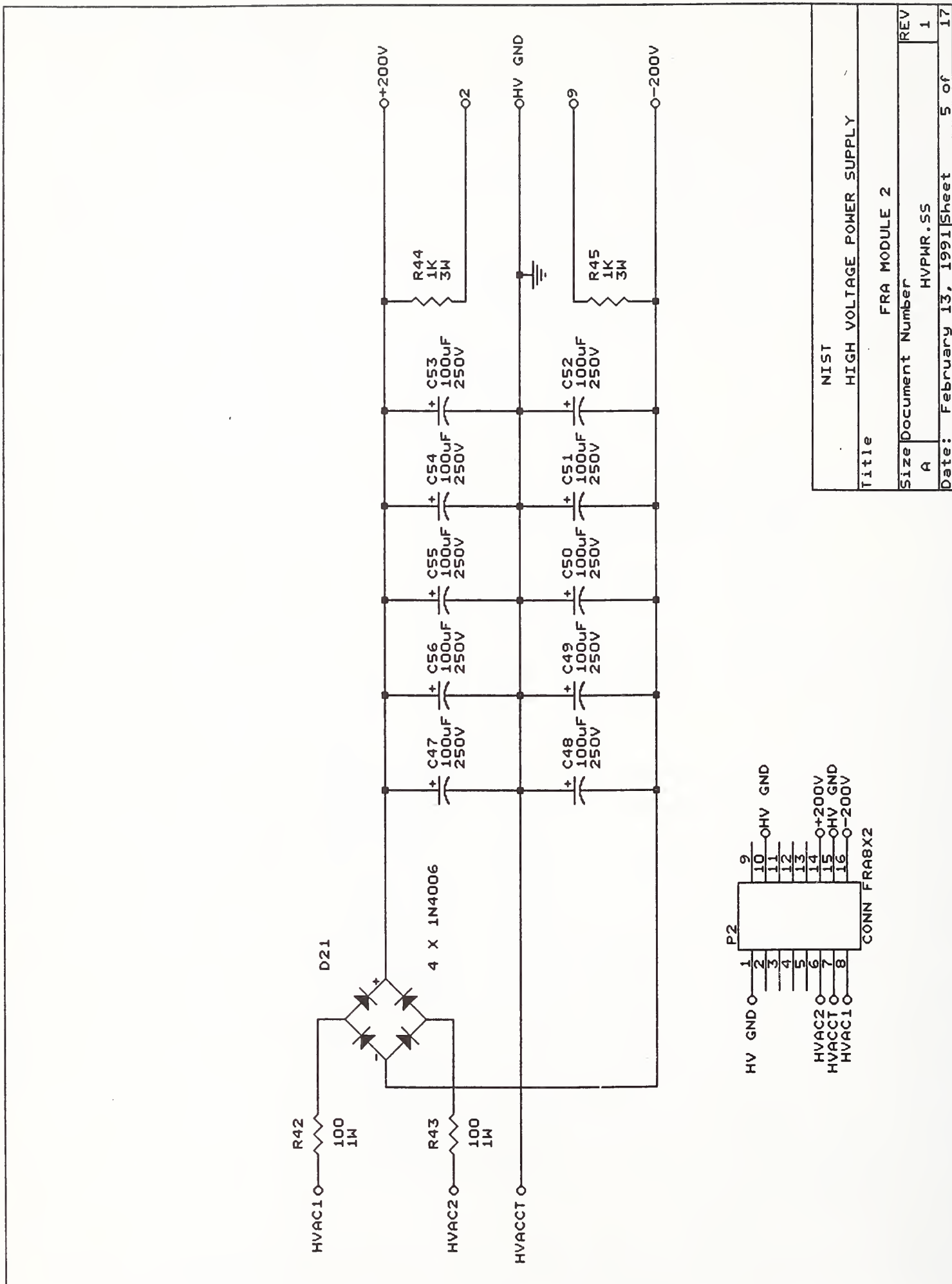


Figure 27. High voltage power supply in module 2, analog box.

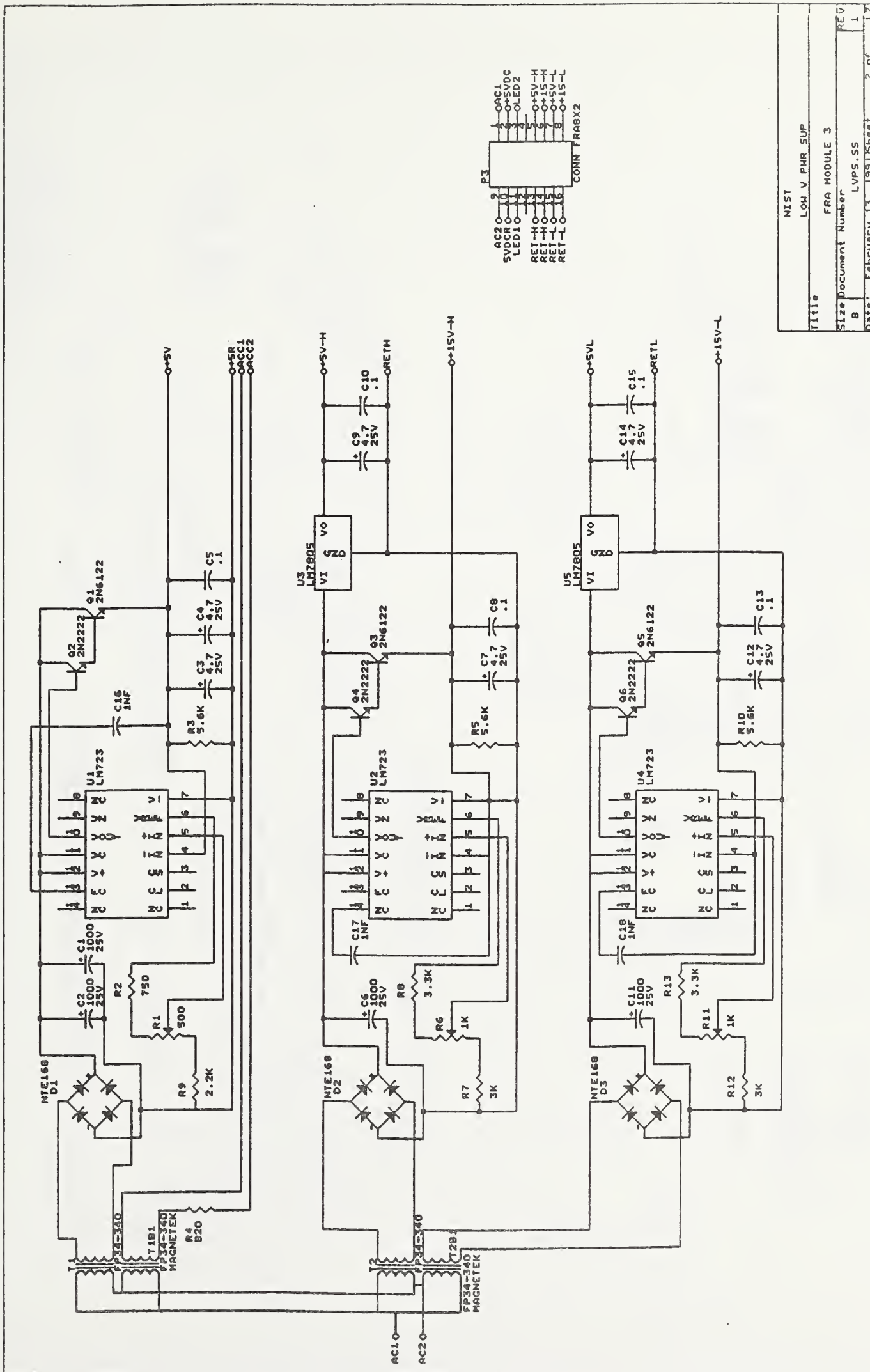
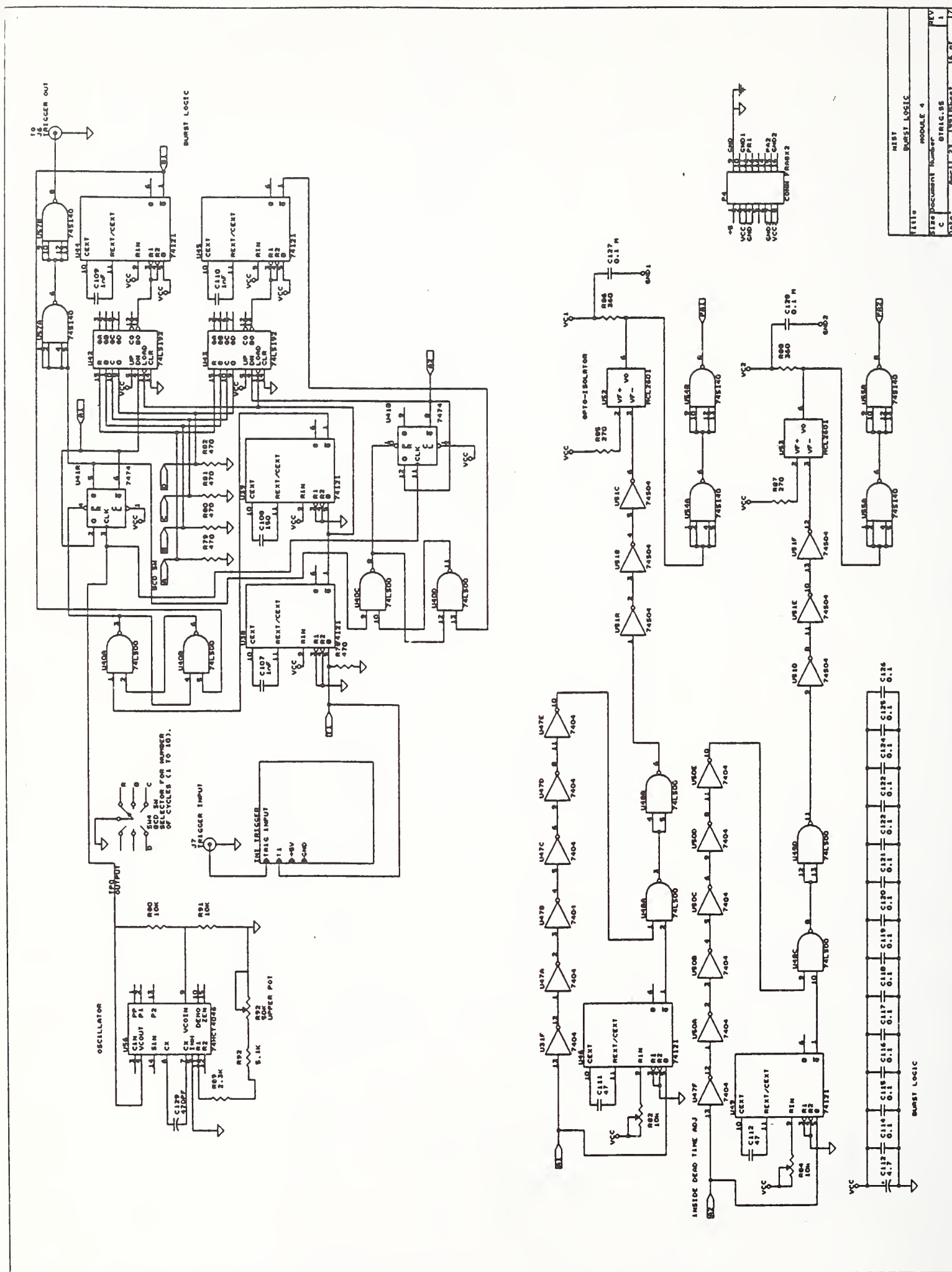
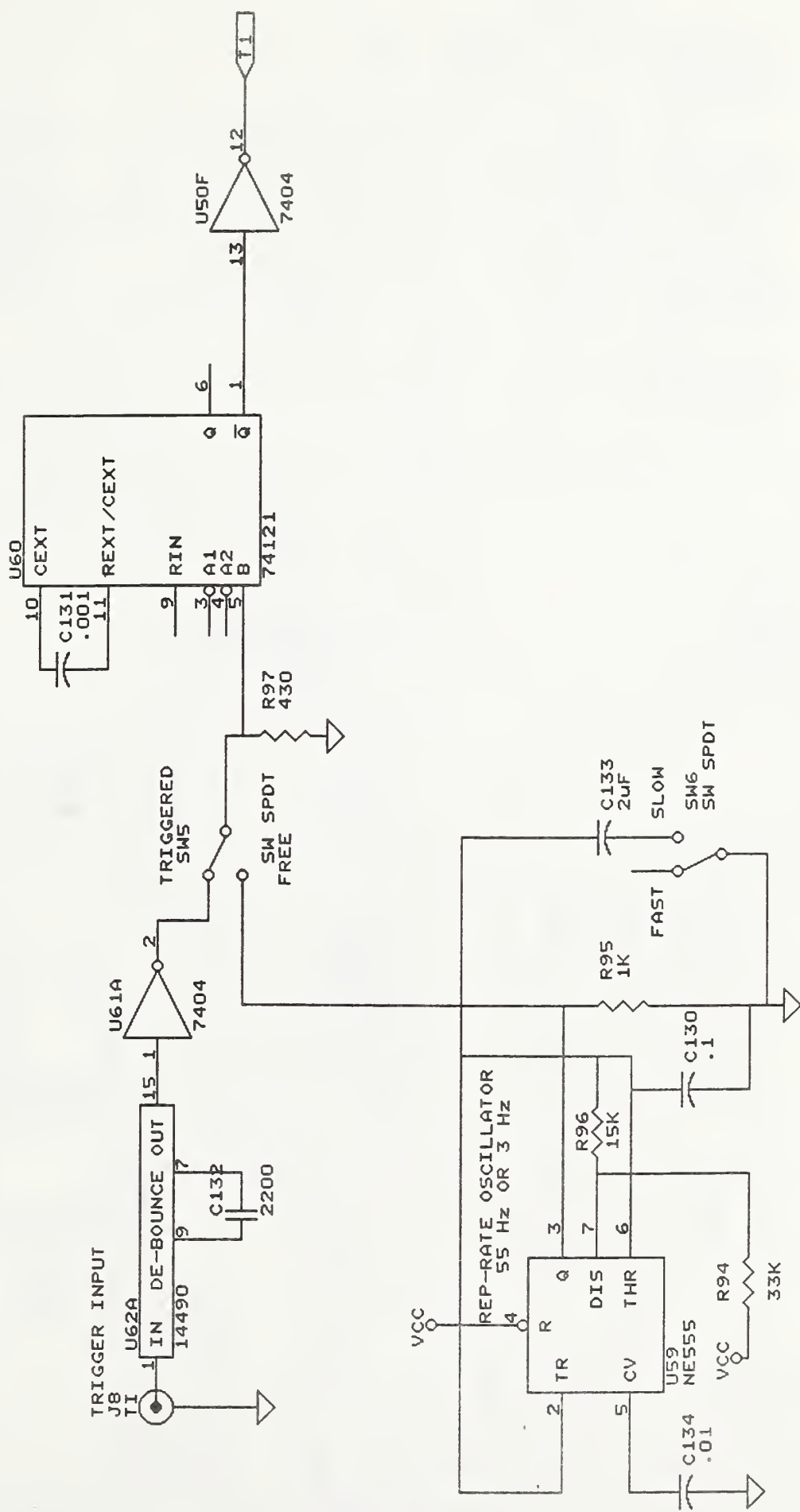


Figure 28. Low voltage power supply in module 3, analog box.



Burst logic in module 4, analog box. See Fig. 29B for the internal trigger circuit.



NIST			
BURST LOGIC TRIGGER			
FRA MODULE 4 MEZ. BD			
Title	Size	Document Number	REV
	A	INTTR.FRA	
Date:	April 23, 1991		Sheet 17 of 17

Figure 29B. Internal trigger for the logic circuit in Fig. 29A.

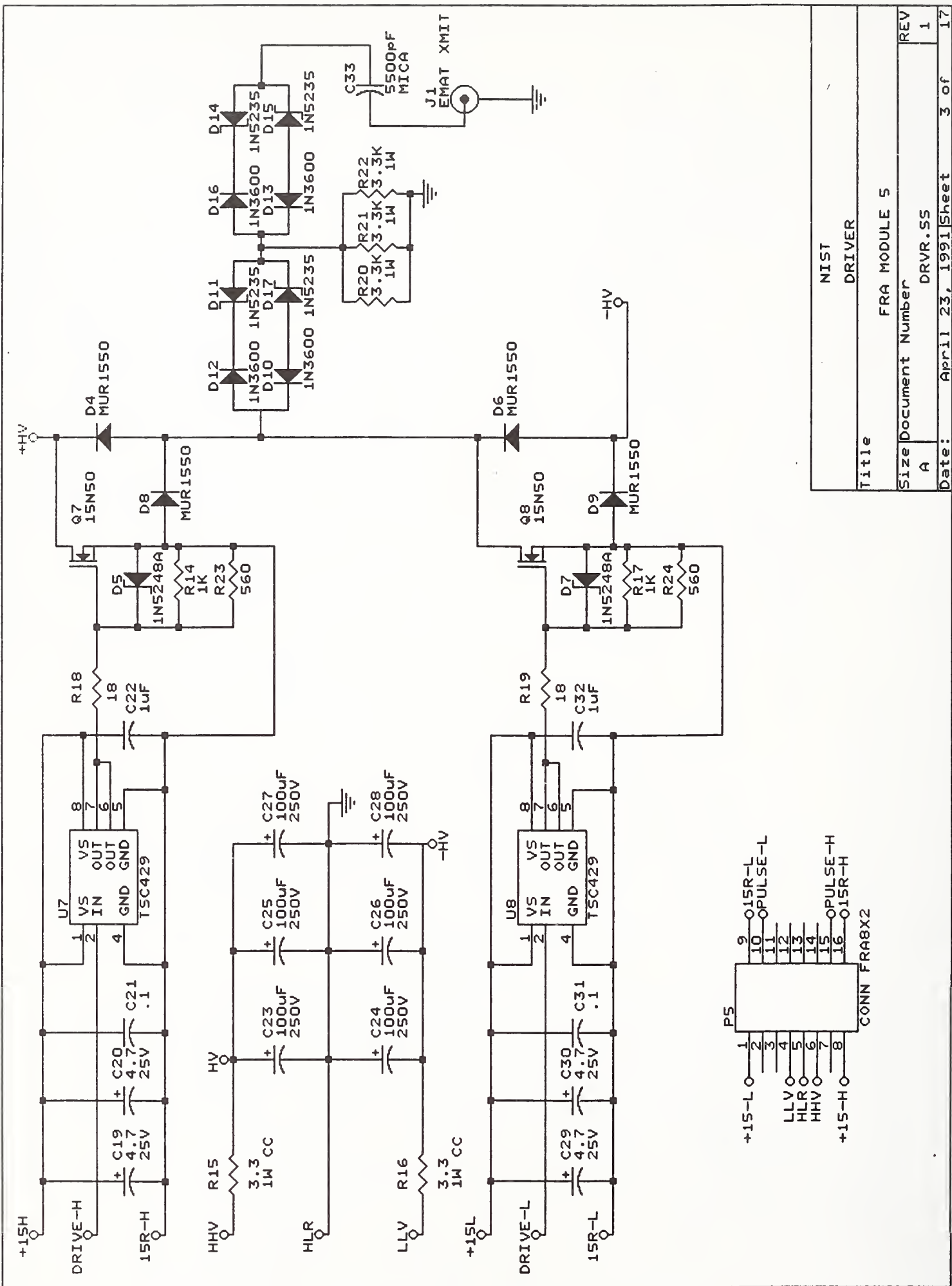


Figure 30. High power driver in module 5, analog box.

Size	A	Document Number	DRV.R.SS	REV
Date:	April 23, 1991	Sheet	3 of 17	1

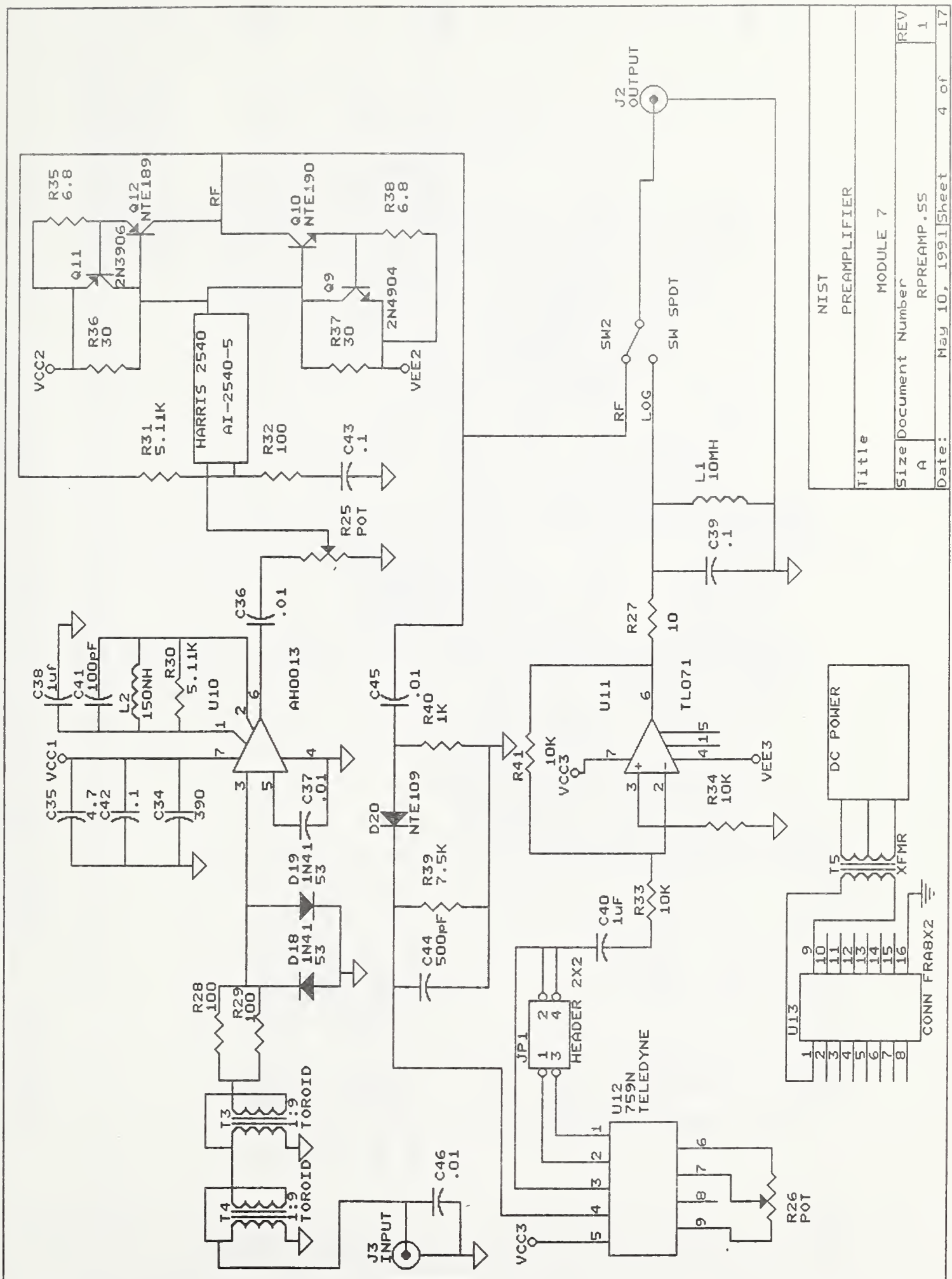
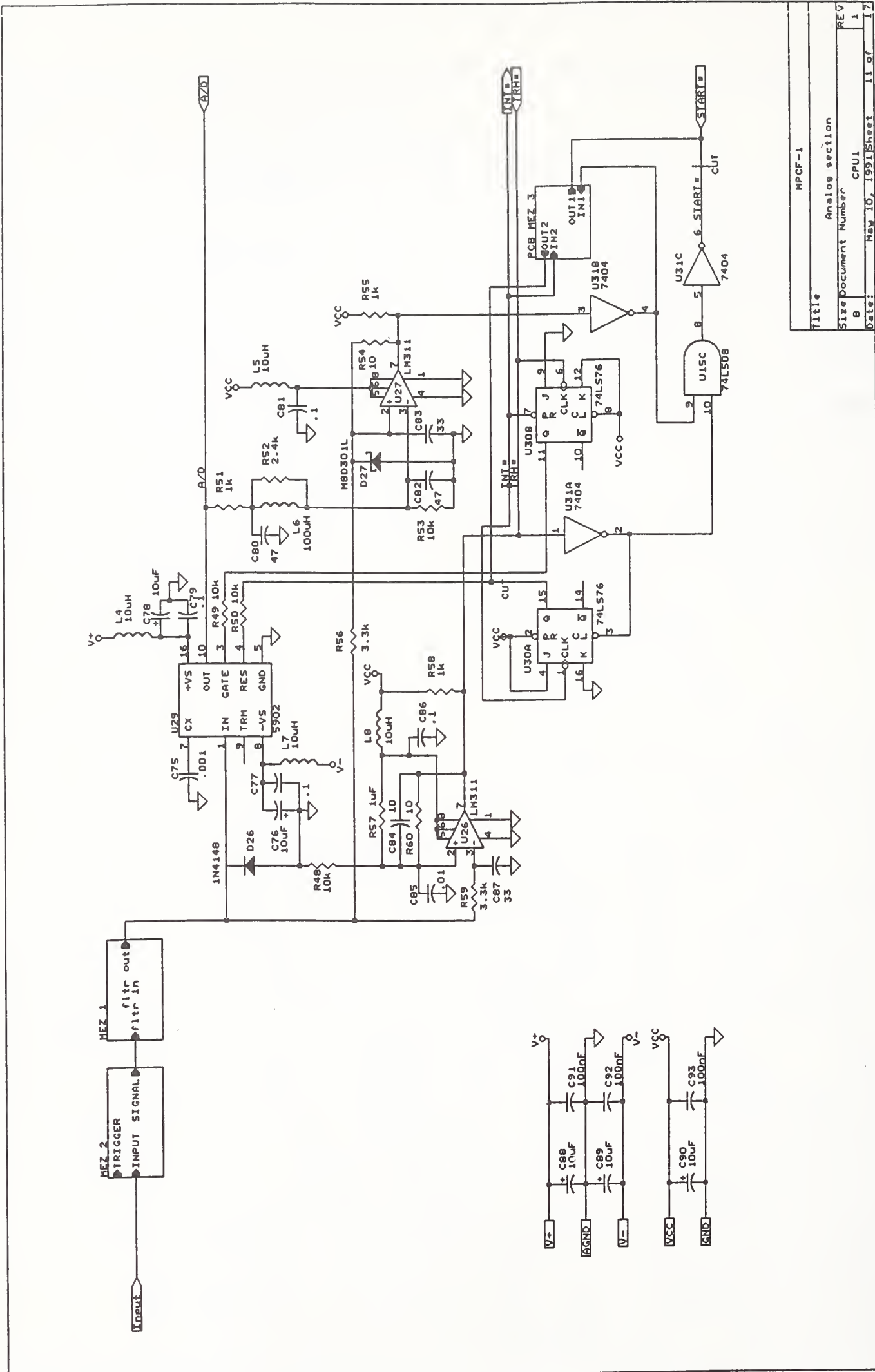


Figure 31. Signal preamplifier in module 7, analog box.



Analog signal processing section of digital box. The circuit of the three mezzanine boards are in Figs. 32 B-D.

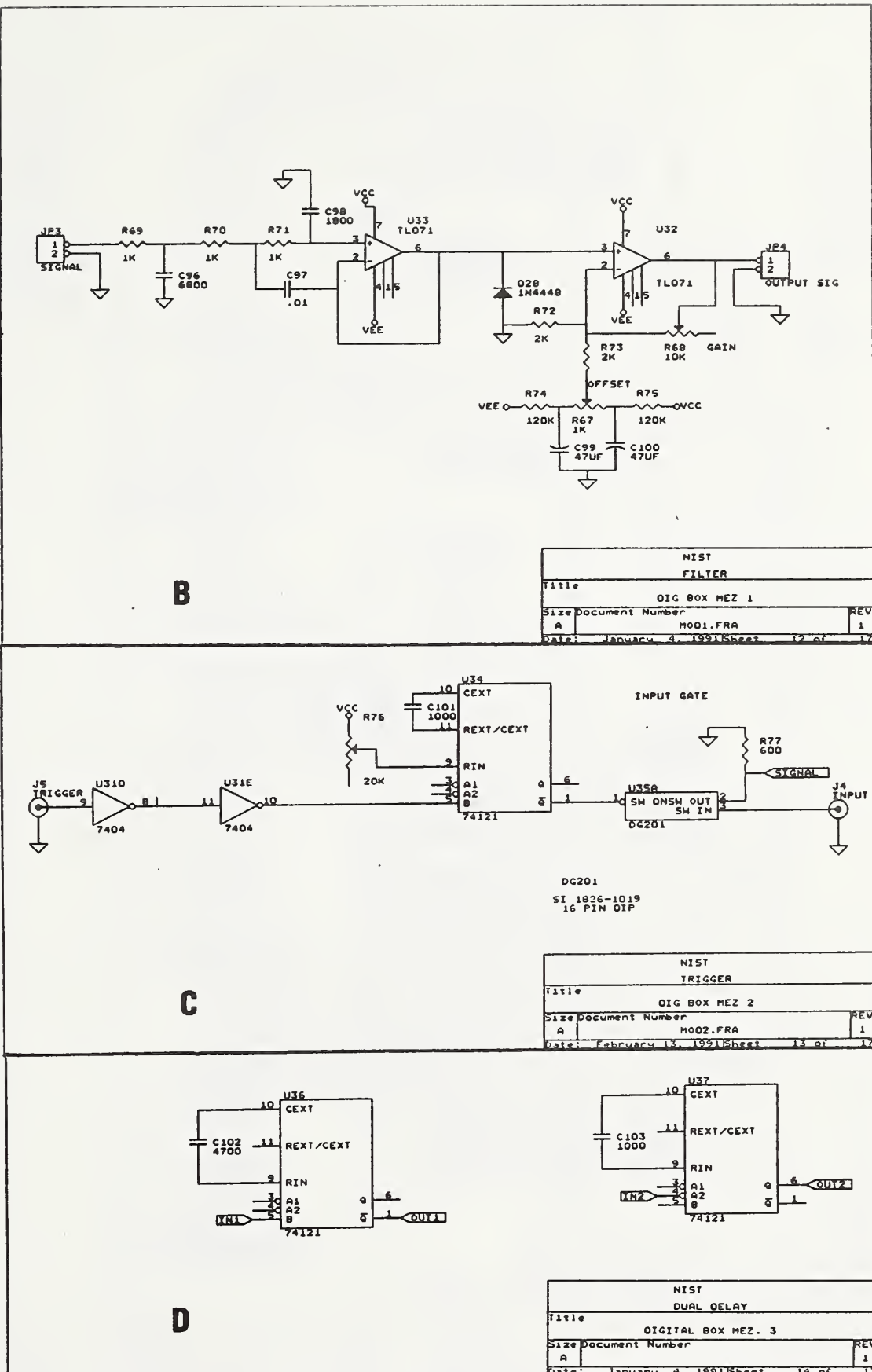


Figure 32. B. Mezzanine board 1. C. Mezzanine board 2. D. Mezzanine board 3. These are plug-ins for the circuit in Fig. 32 A.

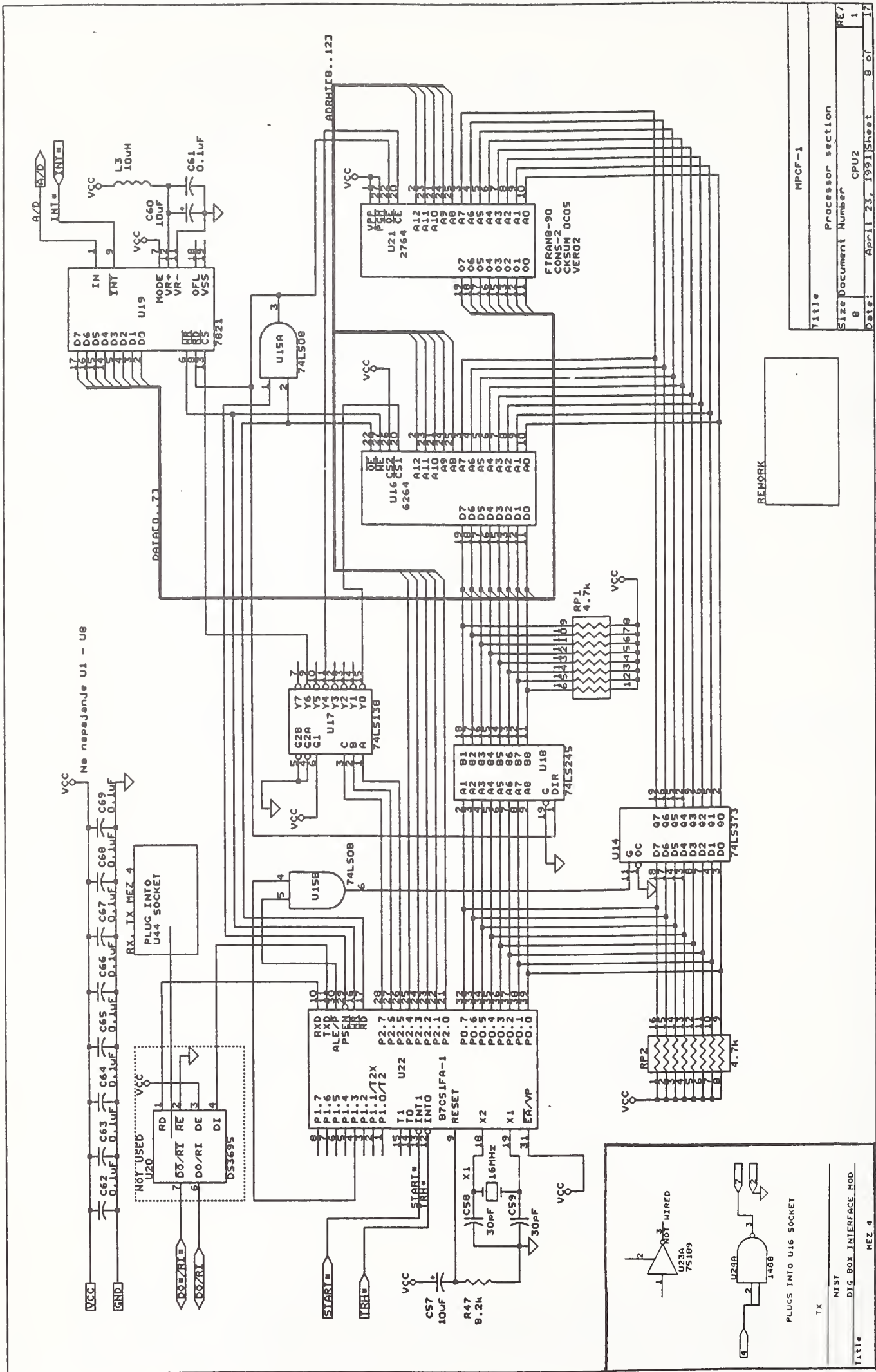


Figure 33. Microprocessor section of digital box.

List of Electronic Components, Analog and Digital Boxes

Item	Quantity	Reference	Part	Item	Quantity	Reference	Part
1	1	SW1	WHEEL SENSING SWITCH	37	1	C36	.01
2	3	U1, U2, U4	LM723	38	6	C37, C45, C46, C85, C97, C134	.01
3	6	C1, C2, C6, C11, C101, C103	1000	39	2	D18, D19	1N41
4	1	R1	500	40	2	R25, R26	POT
5	1	R2	750	41	1	JP1	HEADER 2X2
6	3	R3, R5, R10	5.6K	42	1	L1	10MH
7	12	C3, C4, C7, C9, C12, C14, C19, C20, C29, C30, C35, C113	4.7	43	4	R27, R54, R60, C84	10
8	15	C5, C8, C10, C13, C15, C21, C31, C39, C42, C43, C77, C79, C81, C86, C130	.1	44	1	U12	759N
9	1	R4	820	45	5	R28, R29, R32, R42, R43	100
10	2	U3, U5	LM7805	46	2	R30, R31	5.11K
11	12	R6, R11, R14, R17, R40, R44, R45, R67, R69, R70, R71, R95	1K	47	1	L2	150NH
12	2	R7, R12	3K	48	6	R33, R34, R41, R68, R90, R91	10K
13	6	R8, R13, R20, R21, R22, R89	3.3K	49	2	R35, R38	6.8
14	1	R9	2.2K	50	2	R36, R37	30
15	3	D1, D2, D3	NTE168	51	1	R39	7.5K
16	3	C16, C17, C18	1NF	52	1	D20	NTE109
17	4	T1, T2, T1B1, T2B1	FP34-340	53	1	Q9	2N4904
18	6	P3, P1, P2, P4, P5, U13	CONN FRA8X2	54	1	Q10	NTE190
19	3	Q2, Q4, Q6	2N2222	55	1	Q11	2N3906
20	3	Q1, Q3, Q5	2N6122	56	1	Q12	NTE189
21	2	U7, U8	TSC429	57	2	T3, T4	1:9
22	2	Q7, Q8	15N50	58	3	SW2, SW5, SW6	SW SPDT
23	4	D4, D6, D8, D9	MUR1550	59	1	J2	OUTPUT
24	2	D5, D7	1N5248A	60	2	J3, J4	INPUT
25	2	R15, R16	3.3	61	1	T5	XFMR
26	1	J1	EMAT XMIT	62	1	C44	500pF
27	2	R18, R19	18	63	1	C38	1uF
28	4	D10, D12, D13, D16	1N3600	64	1	C41	100pF
29	4	D11, D14, D15, D17	1N5235	65	1	T6	200KVA
30	2	R23, R24	560	66	1	SW3	POWER
31	4	C22, C32, C40, R57	1uF	67	1	SW5A1	HIGH VOLTAGE
32	1	C33	5500pF	68	2	SW5C1, SW5B1	3P2T
33	16	C28, C23, C24, C25, C26, C27, C47, C48, C49, C50, C51, C52, C53, C54, C55, C56	100uF	69	2	D22, D23	LN28RCP
34	1	U10	AH0013	70	1	R46	12K
35	3	U11, U32, U33	TL071	71	1	D21	4 X 1N4006
36	1	C34	390	72	10	U38, U34, U36, U37, U39, U44, U45, U46, U49, U60	74121
				73	2	U40, U48	74LS00
				74	5	R78, R79, R80, R81, R82	470

List of Electronic Components, Analog and Digital Boxes (cont.)

Item	Quantity	Reference	Part	Item	Quantity	Reference	Part
75	3	C107, C109, C110	1nF	113	2	RP1, RP2	4.7k
76	1	C108	150	114	1	U19	7821
77	1	U41	7474	115	5	L3, L4, L5, L7, L8	10uH
78	2	U42, U43	74LS192	116	9	C61, C62, C63, C64, C65, C66, C67, C68, C69	0.1uF
79	4	U31, U47, U50, U61	7404	117	1	U20	DS3695
80	4	C111, C80, C82, C112	47	118	1	U21	2764
81	6	R83, R48, R49, R50, R53, R84	10k	119	1	X1	16MHz
82	2	R85, R87	270	120	1	U22	87C51FA-1
83	2	C127, C128	0.1 M	121	1	U23	75189
84	2	R86, R88	360	122	1	U24	1488
85	1	U51	74S04	123	2	U26, U27	LM311
86	2	U52, U53	MCL2601	124	1	U29	5902
87	3	U54, U55, U57	74S140	125	1	U30	74LS76
88	1	U56	74HCT4046	126	1	L6	100uH
89	1	C129	470PF	127	3	R51, R55, R58	1k
90	1	R92	5.1K	128	1	R52	2.4k
91	1	R93	50K	129	2	R56, R59	3.3k
92	1	J7	TRIGGER INPUT	130	1	D26	1N4148
93	1	SW4	BCD SW	131	2	C87, C83	33
94	13	C114, C115, C116, C117, C118, C119, C120, C121, C122, C123, C124, C125, C126	0.1	132	3	C91, C92, C93	100nF
95	1	J6	TRIGGER OUT	133	1	D27	MBD301L
96	1	U59	NE555	134	1	U35	DG201
97	1	R94	33K	135	1	R76	20K
98	1	J8	TI	136	1	R77	600
99	1	U62	14490	137	1	J5	TRIGGER
100	1	R96	15K	138	1	C102	4700
101	1	R97	430	139	1	C96	6800
102	1	C132	2200	140	1	C98	1800
103	1	C133	2uF	141	2	R72, R73	2K
104	2	C131, C75	.001	142	2	R74, R75	120K
105	1	U14	74LS373	143	2	C99, C100	47UF
106	7	C57, C60, C76, C78, C88, C89, C90	10uF	144	1	JP3	SIGNAL
107	1	R47	8.2K	145	1	JP4	OUTPUT SIG
108	2	C58, C59	30pF	146	1	D28	1N4448
109	1	U15	74LS08	147	1	T7	INDUSTRIJSKA ELECKTRONI
110	1	U16	6264	148	1	C104	4700/40V
111	1	U17	74LS138	149	2	C105, C106	1K/25V
112	1	U18	74LS245				

SOFTWARE

Operation

The signal processing software within the box of digital electronics is contained in an EPROM. Turning the power switch on activates the microprocessor and its command program.

The computer serving as the report station has two power switches: CPU and monitor. After the booting operation, it is necessary to load the communication and data recording program from the internal hard disk. The simplest way to do this is to enter the command "TRN." This executes a batch file containing two commands:

```
CD TRN  
COMTRN
```

Upon entry, the program needs a name used for the file storing the results.

Enter the file name for storing the data : XXXX

Sequential numbers (starting at 0) and the extension .DAT are added to this name to create a separate file for each train. The screen then clears and displays the name of the file prepared for the data about to be received as well as function commands available (see below). The results from the signal processor (received over the RS-232 interface) are then collected. When the time since the last signal is one minute, the assumption is that the end of the train is passed. The file is closed, its summary presented on the screen, and the next file is prepared. Below is a screen sample:

```
File name : XXXX1.dat  
* Main Results *      F1 or F2 to operate current COM1/2  
Total wheels 4      F3 choose window to look for more  
Good wheels 0      F4 to change the current file name  
No test 0          F5 change the file number to read  
Wheel size 36"     F6 sort and view the file results  
                    PGUP to scroll one page up of data  
                    PGDN to scroll one page down data  
                    Esc you want to terminate program  
  
*** No test ***    ** Poor metal **    ** Many flaws**    ** Deep flaw **  
                    Size 36 Wh# 1  
                    Size 36 Wh# 2  
                    Size 36 Wh# 3  
                    Size 36 Wh# 4
```

This sample is from a laboratory test of one wheel (with an artificial slot) rolled over the EMAT four times. On each pass, the signal processor found the echo from the slot and raised the "Deep Flaw" flag. Note that the data displayed have been recorded on the hard disk in the file XXXX0.DAT; the file XXXX1.DAT (noted on the top line) will receive the data from the next train.

The functional commands always displayed on the screen have several uses:

F1/F2 switch between communication ports 1/2.

F4 allows you to change the file name.

F5 allows you to change the sequence number on the file name.

F6 allows you to examine the data in the file named on the top line.

If a train's passage raises enough flags, it will not be possible to display all the data on one screen.

F3 allows you to select one of the four flags, and see all the data.

PGDN scrolls down through the data.

PGUP scrolls up through the data.

Finally:

ESC exits the program, leaving you in the TRAIN subdirectory.

Program Listings

The first two programs, FTRAIN.C and FTIMER.C, were compiled and linked using Franklin C-Compiler-51. Machine code for these two programs is contained in the EPROM in the digital box.

The third program, COMTRN.C, was compiled in Microsoft Quick C. This is the program in the reporting computer that accepts the test results from the digital box then records them in a file and presents them on the monitor.

FTRAIN.C

```

#include "reg52.h"
#include "stdio.h"
#include "absacc.h"
#define CR 0xd      /* Ascii carriage return value */
#define port 0xc000  /* The A/D converter port address at C000H */
bit start_test;
extern bit timer_flag;
extern bit strt;
extern int cnst;
extern data unsigned int timerl_cnt;
extern data unsigned char count;
data unsigned int wheel_cnt;
char demo;
void init();
void ass_data();
void first_rt();
void second_rt();
void calc_flaw();
void result_flaw();
void tran_data();
void clr_all();
void send_cnt();
data int forever;
void main()
{
    init();
    clr_all();      /* Clear all parameters for the coming test */
    timer_flag=0;
    forever=1;
    while (forever) {           /* Main loop for every test */
        if ((timer_flag == 1) && (count >= 3)) { /* Timer 0 interrupt ocured now process the data
            timer_flag=0;
            ass_data();           /* Organization of the collected data */
            first_rt();          /* Look for first round trip */
            second_rt();          /* Look for second round trip */
            calc_flaw();          /* Calculate and process the flaw signal */
            result_flaw();        /* Assign the size and the flaw results to be transmitted */
            tran_data();          /* Transmit the data to host computer */
            clr_all();            /* Clear all parameters for the coming test */
            demo=XBYTE [port];   /* Read A/D converter for initilization */
            TH0=0xF4;              /* Load count for timer_0 to generate 2ms sampling */
            TLO=0x41;
            timerl_cnt=0;
            wheel_cnt++;
        }
        /* End of timer_0 prosessing */
        if (timerl_cnt >= 1220) { /* One minute pass since the last train */
            if (wheel_cnt != 0) {
                send_cnt();
                wheel_cnt=0;
            }
            timerl_cnt=0;
        }
        /* End of while */
    }

    void init()
    {
        TCON=0x45;           /* Falling edge triggered external interrupts */
        SCON=0x52;           /* Communication 8 bit recieve on & TI is on */
        TMOD=0x11;           /* Timer_0 16 bit timer mode 1, timer_1 16 bit auto reload for real time */
        IP=0x5;               /* Priority for external interrupts */
        TH0=0xF4;              /* Load count for timer_0 to generate 2ms sampling */
        TLO=0x41;
        TH1=TL1=0;            /* Generate 65536 cycles for real time timer_1 */
        demo=XBYTE [port];   /* Read A/D converter for initilization */
        RSO=RS1=0;             /* Working area bank 0 for R0, R7*/
        IE=0x8F;
        timerl_cnt=0;          /* Opareting timer 1 as a real time as a timer in internal */
        /* mode due to 12Mhz every 15.25 timerl_cnt - 1 sec */
        RCAP2H=0xff;           /* Time setting for a Baud Rate generator of 9600 */
        RCAP2L=0xcb;           /* on timer two for RS - 232 communication */
        T2CON=0x30;            /* Baud rate generator of 9600 to serial port */
        TR2=1;
        TR1=1;                 /* Timer 1 is running as a real time clock */
        DPH=0xc0;
        DPL=0x00;
        P2=0;
        cnst=2;                /* The constant that determines the deep of the flaw */
        start_test=1;
        wheel_cnt=0;
    }
}

```

END

FTIMER.C

```

#include "reg51.h"
#include "stdio.h"
#define CR 0xd          /* Ascii carriage return value */
bit strt;
bit timer_flag;
bit srtrip_ok;
bit deep_flaw, many_flaw;
int srtrip_num;
int frtrip_num;
int cnst;
char wheel_size;
data unsigned char count;
data unsigned char low_byte[20], high_byte[20];
data unsigned char read_peak[20];
unsigned int frtrip;
unsigned int rtrip;
unsigned char frtrip_amp, srtrip_amp;
data unsigned char flaw_size;
union tim_value
{
    unsigned int i_read;
    unsigned char r_value[2];
} u;
struct read_data
{
    unsigned int time_read[20];
    unsigned char peak_read[20];
    unsigned char decision[20];
} d;
void ass_data()
{
    char i;
    for ( i=0; i<=count; i++ ) {
        u.r_value[1]=low_byte[i];
        u.r_value[0]=high_byte[i];
        d.time_read[i]=u.i_read;
        d.peak_read[i]=read_peak[i];
    }
}

void first_rt()      /* This procedure searches for 1 round trip */
{
    int i;
    unsigned char max_amp=0;          /* Look for the maximum amplitude also Dec 4 */
    frtrip=0;
    for ( i=1; i<=count; i++ ) {
        rtrip=d.time_read[i]-d.time_read[0];
        /* Look for first round trip for 28" wheel 720 ± 40 is */
        if ( (rtrip >= 906) && (rtrip <= 1013) && (d.peak_read[i] >= max_amp) )  {
            max_amp=d.peak_read[i];
            frtrip=rtrip;
            d.decision[i]=1;
            frtrip_num=i;
        }                                /* End of 28" wheel */
        /* Look for first round trip for 33" wheel 840 ± 40 is */
        if ( (rtrip >= 1066) && (rtrip <= 1173) && (d.peak_read[i] >= max_amp) )  {
            max_amp=d.peak_read[i];
            frtrip=rtrip;
            d.decision[i]=2;
            frtrip_num=i;
        }                                /* End of 33" wheel */
        /* Look for first round trip for 36" wheel 920 - 40 & +60 is */
        if ( (rtrip >= 1174) && (rtrip <= 1306) && (d.peak_read[i] >= max_amp) )  {
            max_amp=d.peak_read[i];
            frtrip=rtrip;
            d.decision[i]=3;
            frtrip_num=i;
        }                                /* End of 36" wheel */
    }
    frtrip_amp=d.peak_read[frtrip_num]; /* Amplitude of first round trip */
} /* End of first round trip search */

void second_rt()      /* This procedure searches for 2 round trip */
{
    /* The timing of first RT multi. by 2 ± 20 is */
    unsigned int srtrip;
    int i;
    srtrip_ok=0;
    srtrip=frtrip*2;
    for ( i=1; i<=count; i++ ) {
        rtrip=d.time_read[i]-d.time_read[0];
    }
}

```



```

FTIMER.C (cont.)
if ( (rtrip >= srtrip-26) && (rtrip <= srtrip+26) ) {
    srtrip_num=1;
    srtrip_ok=1;
    break;
}
)
wheel_size=d.decision[frtrip_num];
srtrip_amp=d.peak_read[srtrip_num]; /* Amplitude of second round trip */
) /* End of second round trip search */

void calc_flaw()
{
int j;
int prop_amp = 0;
char flaw_num = 0;
prop_amp=(frtrip_amp*cnst)/10; /* Constant of 20% of first RT to evaluate a Deep Flaw */
for ( j=1; j<frtrip_num; j++ ) {
    rtrip=d.time_read[j]-d.time_read[0];
    if ( (rtrip <= 200) ) /* Skip deadtime of 150ls for signal recovery */
        continue;
    }
else {
    flaw_num++;
    if ( d.peak_read[j] >= prop_amp ) deep_flaw=1;
    if ( flaw_num >= 3 ) many_flaw = 1;
    }
}
) /* End of calculation the flaw signals */

void result_flaw()
{
if ( frtrip == 0 ) /* There is no first round trip */
    wheel_size='0';
    flaw_size='1';
)
if ( srtrip_ok == 1 ) /* There were a second round trip */
    wheel_size=wheel_size+0x40;
    if ( deep_flaw == 1 ) flaw_size='3';
    if ( many_flaw == 1 ) flaw_size='4';
    if ( ( deep_flaw == 0 ) && ( many_flaw == 0 ) ) flaw_size='5';
)
if ( ( srtrip_ok == 0 ) && ( frtrip != 0 ) ) /* There is no second round trip means poor metal */
    wheel_size=wheel_size+0x40;
    flaw_size='2';
)
)

void tran_data()
{
    while(!TI); /* Transmit the wheel size first */
    TI=0;
    SBUF=wheel_size;
    while(!TI); /* Transmit the flaw report second */
    TI=0;
    SBUF=flaw_size;
    while(!TI); /* Transmit the CR to end transmission */
    TI=0;
    SBUF=CR;
)
}

void clr_all()
{
    strt=0;
    deep_flaw=0;
    many_flaw=0;
    srtrip_num=0;
    frtrip_num=0;
    wheel_size=0;
    flaw_size=0;
    rtrip=0;
    frtrip_amp=0;
    srtrip_amp=0;
)
}

timer0() interrupt 1 using 0
{
    EA=0;
    timer_flag=1;
    TR0=0;
    EA=1;
)

```

END

COMTRN.C

```

#include <dos.h>
#include <malloc.h>
#include <stdio.h>
#include <stdlib.h>
#include <time.h>
#include <conio.h>
#include <bios.h>
#include <graph.h>

#define COM1 0
#define COM2 1
#define F1 0x3b
#define F2 0x3c
#define F3 0x3d
#define F4 0x3e
#define F5 0x3f
#define F6 0x40
#define F7 0x41
#define F8 0x42
#define F9 0x43
#define F10 0x44
#define CURUP 0x48
#define CURDN 0x50
#define PGUP 0x49
#define PGDN 0x51
#define Esc 0x1
#define EOI 0x20
#define peek( addr )      (*(unsigned char far *)addr)

/* Stack and pointer checking off */
#pragma check_stack( off )
#pragma check_pointer( off )
enum BOOLEAN { FALSE, TRUE };

/* Prototypes for interrupt functions */
void (interrupt far *oldcomun1)( void );
void (interrupt far *oldcomun2)( void );
void interrupt far newcomun1( void );
void interrupt far newcomun2( void );

int read_flag = FALSE;
char data_in[1000], data_read[1000];
char *data_ptr;
int count, count1, forever=1;
char key_press,buffer[1000];
struct videoconfig vc;
int com2_set=0, com2_on=0, file_num=0;
unsigned char old_int_cont, new_int_cont;
char nam_file[17], nam_file_in[10];
char data_end[] = "NUM = ";
char *str_find_ptr;
int wheel_count, good_wheel, wheel_size;
char seps[] = "\r\n";
struct wheel_info
{
    char info[3];
    char size;
    char flaw;
} wheel[1000];
int no_test1,deep_flaw1,poor_metal1,many_flaw1;
int no_test[1000],deep_flaw[1000],poor_metal[1000],many_flaw[1000];
int i, whe_size, pgup=0, pgdn=0;
char choose_wdo;
int page_tot, page_nub_n, page_nub_p, page_nub_m, page_nub_d;

main( )
{
    unsigned key, scan;
    int kread = _KEYBRD_READ;
    int kready = _KEYBRD_READY;
    int kshiftstatus = _KEYBRD_SHIFTSTATUS;

    /* If bit 4 of the byte at 0x0040:0x0096 is set, the new keyboard is present */
    if( peek( 0x00400096 ) & 0x10 )
    {

```



COMTRN.C (cont.)

```

        kread = _NKEYBRD_READ;
        kready = _NKEYBRD_READY;
        kshiftstatus = _NKEYBRD_SHIFTSTATUS;
    }
    count=count1=0;
    init_com1();
    _getvideoconfig( &vc );
    _setvideoemode( _TEXT80 );
    system( "cls" );
    name_file();
    new_file();
    _settextwindow( 3, 22, 11, 57 );
    _settextcolor(0);
    _setbkcolor(11L);
    sprintf(buffer," F1 or F2 to operate current COM1/2 ");
    _outtext( buffer );
    sprintf(buffer," F3 choose window to look for more ");
    _outtext( buffer );
    sprintf(buffer," F4 to change the current file name ");
    _outtext( buffer );
    sprintf(buffer," F5 change the file number to read ");
    _outtext( buffer );
    sprintf(buffer," F6 sort and view the file results ");
    _outtext( buffer );
    sprintf(buffer," PGUP to scroll one page up of data ");
    _outtext( buffer );
    sprintf(buffer," PGDN to scroll one page down data ");
    _outtext( buffer );
    sprintf(buffer," Esc you want to terminate program ");
    _outtext( buffer );
    while ( forever )
    {
        str_find_ptr=data_in;
        str_find_ptr=strstr( str_find_ptr, data_end );
        if ( str_find_ptr != NULL ) {
            str_find_ptr=strchr( str_find_ptr, 13 );
            if ( ( str_find_ptr != NULL ) && ( read_flag ) ) {
                read_flag= FALSE;
                putchar(7);
                putchar(7);
                putchar(7);
                putchar(7);
                putchar(7);
                save_file();
                count=0;
                read_file();
                sort_data();
                view_data();
                file_num++;
                new_file();
            }
        }
        while( 1 ) {
            if ( _bios_keybrd( kready ) ) break;
            if ( read_flag ) {
                if ( !( _bios_keybrd( kready ) ) ) {
                    scan=0;
                    goto cont;
                }
            }
        }
        /* _bios_keybrd( kread ); */
        key = _bios_keybrd( kread );
        scan = key >> 8;
        cont:
        switch( scan )
        {
        case F3:
            change_window();
            break;
        case PGDN:
            pgdn=1;
            select_window();
            break;
        case PGUP:
    }
}

```

COMTRN.C (cont.)

```

pgup=1;
select_window();
break;
case F4:
name_file();
new_file();
break;
case F5:
change_num();
new_file();
break;
case F6:
read_file();
sort_data();
view_data();
break;
case F1:
com2_set=0;
init_com1();
break;
case F2:
init_com2();
break;
case Esc:
if ( com2_on) {
_dos_setvect( 0x0b, oldcomun2 );
_dos_setvect( 0x0c, oldcomun1 );
outp(0x21, old_int_cont);
_setvideomode(_DEFAULTMODE);
exit(1);
break;
default:
break;
}
}
}
init_com1()
{
unsigned char dlab;
_bios_serialcom( _COM_INIT,COM1,_COM_CHR8 | _COM_STOP1 | _COM_NOPARITY | _COM_9600 );
oldcomun1 = _dos_getvect( 0x0c ); /* Changing the comun. intr. handler */
_dos_setvect( 0x0c, newcomun1 );
dlab=(inp(0x3fb) & 0x7f); /* Read dlab bit from line control register enables intr. */
outp(0x3fb,dlab); /* Set dlab=0 for fourther communication handling */
outp(0x3f9,0x01); /* Enable receive data interrupt */
outp(0x20,0x4a);
old_int_cont=inp(0x21);
outp(0x21,(old_int_cont & 0xef));
outp(0x3fc,0x0b); /* Set out2 in modem control register enables intr. */
}
init_com2()
{
unsigned char dlab;
_bios_serialcom( _COM_INIT,COM2,_COM_CHR8 | _COM_STOP1 | _COM_NOPARITY | _COM_9600 );
oldcomun2 = _dos_getvect( 0x0b ); /* Changing the comun. intr. handler */
_dos_setvect( 0x0b, newcomun2 );
dlab=(inp(0x2fb) & 0x7f); /* Read dlab bit from line control register enables intr. */
outp(0x2fb,dlab); /* Set dlab=0 for fourther communication handling */
outp(0x2f9,0x01); /* Enable receive data interrupt */
com2_set=0x100;
outp(0x21,(old_int_cont & 0xf7));
com2_on=1;
outp(0x2fc,0x0b); /* Set out2 in modem control register enables intr. */
}
name_file()
{
_settextwindow( 24,14, 25, 66);
_settextcolor(0);
_setbkcolor(11L);
_clearscreen( _GWINDOW );
sprintf(buffer," Enter file name for storing the data into : ");

}

```

COMTRN.C (cont.)

```
_outtext( buffer );
scanf("%s",nam_file_in);
_setbkcolor(0L);
_clearscreen( _GWINDOW );
}

change_num()
{
    _settextwindow( 24,26, 25, 54);
    _settextcolor(0);
    _setbkcolor(11L);
    sprintf(buffer," Enter a new file number :   ");
    _outtext( buffer );
    _settextposition(1,28);
    scanf("%d", &file_num);
    _setbkcolor(0L);
    _clearscreen( _GWINDOW );
}

new_file()
{
char strg[3];
    itoa(file_num,strg,10);
    nam_file[0]='\0';
    strcat(nam_file, nam_file_in);
    strcat(nam_file, strg);
    strcat(nam_file, ".dat");
    _settextwindow( 2, 29, 2, 53);
    _setbkcolor(0L);
    _clearscreen( _GWINDOW );
    _settextcolor(7);
    _setbkcolor(13L);
    _settextposition(0,0);
    sprintf(buffer," File name : %s ",nam_file);
    _outtext( buffer );
}

read_file()
{
FILE *file_in;
    if( (file_in=fopen(nam_file, "rb" )) == NULL )
    {
        printf( "Can't open input file" );
        exit( 1 );
    }

    data_ptr=data_read;
    while( !feof( file_in ) )
    {
        *data_ptr=fgetc( file_in );
        data_ptr++;
    }
    fclose( file_in );
}

save_file()
{
FILE *file_out;
    if( (file_out=fopen(nam_file, "wb" )) == NULL )
    {
        printf( "Can't open input file" );
        exit( 1 );
    }
    for ( i=0; i<=count; i++ ) {
        fputc( data_in[i], file_out );
    }
    fclose( file_out );
}

change_window()
{
    _settextwindow( 24,13, 25, 68);
    _settextcolor(0);
    _setbkcolor(11L);
}
```



COMTRN.C (cont.)

```

sprintf(buffer," Type 'n', 'p', 'm' or 'd' to choose current window ");
_outtext( buffer );
_settextposition(0,53);
choose_wdo=getche();
_setbkcolor(0L);
_clearscreen( _GWINDOW );
}
view_data()
{
    page_nub_n=page_nub_p=page_nub_m=page_nub_d=0;
_settextwindow( 4, 2, 9, 20);
_settextcolor(0);
_setbkcolor(10L);
_clearscreen( _GWINDOW );
_setbkcolor(13L);
sprintf(buffer," * Main Results * ");
_outtext( buffer );
_setbkcolor(10L);
_settextposition(2,0);
sprintf(buffer," Total wheels  %3d ",wheel_count);
_outtext( buffer );
_settextposition(3,0);
sprintf(buffer," Good wheels  %3d ",good_wheel);
_outtext( buffer );
_settextposition(4,0);
sprintf(buffer," No test  .  %3d ",no_test1);
_outtext( buffer );
_settextposition(5,0);
sprintf(buffer," Wheel size  %d\" ",wheel_size);
_outtext( buffer );
view_no();
view_poor();
view_many();
view_deep();
}
view_no()
{
_settextwindow( 12, 3, 23, 19);
_settextcolor(7);
_setbkcolor(15L);
_clearscreen( _GWINDOW );
_setbkcolor(9L);
sprintf(buffer," *** No test *** ");
_outtext( buffer );
_setbkcolor(15L);
_settextcolor(4);
_settextposition(2,0);
page_tot=(no_test1/10)+1;
if ( (page_tot > 1) && ( pgdn || pgup ) ) {
if ( pgdn ) {
pgdn=0;
page_nub_n++;
if ( page_nub_n >= page_tot ) page_nub_n-- ;
}
else {
if ( pgup ) {
pgup=0;
page_nub_n--;
if ( page_nub_n < 0 ) page_nub_n=0;
}
}
}
for ( i=page_nub_n*10+1; i<= 10*(page_nub_n+1) ; i++ ) {
if ( i > no_test1 ) break;
sprintf(buffer," Wheel numb. %3d ", no_test[i]);
_outtext( buffer );
}
if ( i < no_test1 ) {
_settextposition(12,2);
_settextcolor(0);
_setbkcolor(14L);
sprintf(buffer,"** More data **");
_outtext( buffer );
}
}

```



COMTRN.C (cont.)

```
    }

    view_poor()
    {
        _settextwindow( 12, 22, 23, 38);
        _settextcolor(7);
        _setbkcolor(15L);
        _clearscreen( _GWINDOW );
        _setbkcolor(9L);
        sprintf(buffer,"** Poor metal ** ");
        _outtext( buffer );
        _setbkcolor(15L);
        _settextcolor(4);
        _settextposition(2,0);
        page_tot=(poor_metal1/10)+1;
        if ( (page_tot > 1) && ( pgdn || pgup ) ) {
            if ( pgdn ) {
                pgdn=0;
                page_nub_p++;
                if ( page_nub_p >= page_tot ) page_nub_p--;
            }
            else {
                if ( pgup ) {
                    pgup=0;
                    page_nub_p--;
                    if ( page_nub_p < 0 ) page_nub_p=0;
                }
            }
        }
        for ( i=page_nub_p*10+1; i<= 10*(page_nub_p+1) ; i++ ) {
            if ( i > poor_metal1 ) break;
            whe_size=28+((wheel[poor_metal[i]].size)-0x41)*4;
            sprintf(buffer," Size %2d Wh# %3d ",whe_size, poor_metal[i]);
            _outtext( buffer );
        }
        if ( i < poor_metal1 ) {
            _settextposition(12,2);
            _settextcolor(0);
            _setbkcolor(14L);
            sprintf(buffer,"** More data **");
            _outtext( buffer );
        }
    }

    view_many()
    {
        _settextwindow( 12, 41, 23, 57);
        _settextcolor(7);
        _setbkcolor(15L);
        _clearscreen( _GWINDOW );
        _setbkcolor(9L);
        sprintf(buffer," ** Many flaws** ");
        _outtext( buffer );
        _settextcolor(4);
        _setbkcolor(15L);
        _settextposition(2,0);
        page_tot=(many_flaw1/10)+1;
        if ( (page_tot > 1) && ( pgdn || pgup ) ) {
            if ( pgdn ) {
                pgdn=0;
                page_nub_m++;
                if ( page_nub_m >= page_tot ) page_nub_m--;
            }
            else {
                if ( pgup ) {
                    pgup=0;
                    page_nub_m--;
                    if ( page_nub_m < 0 ) page_nub_m=0;
                }
            }
        }
        for ( i=page_nub_m*10+1; i<= 10*(page_nub_m+1) ; i++ ) {
            if ( i > many_flaw1 ) break;
    }
```



COMTRN.C (cont.)

```

whe_size=28+((wheel[many_flaw[i]].size)-0x41)*4;
sprintf(buffer," Size %2d Wh# %3d ",whe_size, many_flaw[i]);
_outtext( buffer );
}
if ( i < many_flaw1 ) {
_settextposition(12,2);
_settextcolor(0);
_setbkcolor(14L);
sprintf(buffer,"** More data **");
_outtext( buffer );
}
}

view_deep()
{
    _settextwindow( 12, 60, 23, 76);
    _settextcolor(7);
    _setbkcolor(15L);
    _clearscreen( _GWINDOW );
    _setbkcolor(9L);
    sprintf(buffer," ** Deep flaw ** ");
    _outtext( buffer );
    _settextcolor(4);
    _setbkcolor(15L);
    _settextposition(2,0);
    page_tot=(deep_flaw1/10)+1;
    if ( (page_tot > 1) && ( pgdn || pgup ) ) {
    if ( pgdn ) {
    pgdn=0;
    page_nub_d++;
    if ( page_nub_d >= page_tot ) page_nub_d--;
    }
    else {
    if ( pgup ) {
    pgup=0;
    page_nub_d--;
    if ( page_nub_d < 0 ) page_nub_d=0;
    }
    }
    for ( i=page_nub_d*10+1; i<= 10*(page_nub_d+1) ; i++ ) {
    if ( i > deep_flaw1 ) break;
    whe_size=28+((wheel[deep_flaw[i]].size)-0x41)*4;
    sprintf(buffer," Size %2d Wh# %3d ",whe_size, deep_flaw[i]);
    _outtext( buffer );
    }
    if ( i < deep_flaw1 ) {
    _settextposition(12,2);
    _settextcolor(0);
    _setbkcolor(14L);
    sprintf(buffer,"** More data **");
    _outtext( buffer );
    }
}
}

select_window()
{
    if ( choose_wdo == 'n' || choose_wdo == 'N' ) view_no();
    if ( choose_wdo == 'p' || choose_wdo == 'P' ) view_poor();
    if ( choose_wdo == 'm' || choose_wdo == 'M' ) view_many();
    if ( choose_wdo == 'd' || choose_wdo == 'D' ) view_deep();
}

sort_data()
{
int num_a,num_b,num_c,max_value;
int i;
char *num_str;
    num_str=data_read;
    num_str+=strcspn( num_str, data_end );
    num_str+=strspn( num_str, data_end );
    num_str=strtok(num_str,seps);
    wheel_count=atoi(num_str);
    num_str=data_read;
}

```



COMTRN.C (cont.)

```

num_str=strtok(data_read,seps);
for ( i=1; i<=wheel_count; i++)  {
wheel[i].size=*num_str;
wheel[i].flaw=(num_str+1);
num_str=strtok(NULL,seps);
}
num_a=num_b=num_c=0;
for ( i=1; i<=wheel_count; i++)  {
if ( wheel[i].size=='A') num_a++;
if ( wheel[i].size=='B') num_b++;
if ( wheel[i].size=='C') num_c++;
}
max_value=max( num_a, num_b );
max_value=max( max_value, num_c );
if(max_value==num_a) wheel_size=28;
if(max_value==num_b) wheel_size=32;
if(max_value==num_c) wheel_size=36;
no_testl=deep_flawl=poor_metal1=many_flawl=good_wheel=0;
for ( i=1; i<=wheel_count; i++)  {
if ( wheel[i].flaw=='1' )  {
no_testl++;
no_test[no_testl]=i;
}
if ( wheel[i].flaw=='2' )  {
poor_metal1++;
poor_metal[poor_metal1]=i;
}
if ( wheel[i].flaw=='3' )  {
deep_flawl++;
deep_flaw[deep_flawl]=i;
}
if ( wheel[i].flaw=='4' )  {
many_flawl++;
many_flaw[many_flawl]=i;
}
if ( wheel[i].flaw=='5' ) good_wheel++;
}
if ( no_testl > 11 ) choose_wdo = 'n';
if ( poor_metal1 > 11 ) choose_wdo = 'p';
if ( many_flawl > 11 ) choose_wdo = 'm';
if ( deep_flawl > 11 ) choose_wdo = 'd';
}

void interrupt far newcomnl()
{
char iir;
iir=(inp(0x3fa) & 7);
if( iir == 4 )
{
    data_in[count+1]='\0';
    read_flag=TRUE;
    data_in[count]=inp( 0x3f8);
    count++;
    outp(0x20,EOI); /* End of interrupt to 8259 */
}
}

void interrupt far newcomn2()
{
char iirl;
iirl=(inp(0x2fa) & 7);
if( iirl == 4 )
{
    data_in[count+1]='\0';
    read_flag=TRUE;
    data_in[count]=inp( 0x2f8);
    count++;
    outp(0x20,EOI); /* End of interrupt to 8259 */
}
}

```

END

CHECKLIST

1. EMAT installed in track
2. Coil package position adjusted horizontally and vertically.
3. All connecting cables (coaxial cables, RS-232) installed
4. Ground clips on both ends of track cable connected.
5. All electronics powered on
6. Reporting computer booted-up and control program loaded

TROUBLE SHOOTING

Some potential problems with possible solutions include:

1. No trigger
Check trigger cable - use multimeter to make sure switch is closing when pressure is applied to coil package (have someone step on the transducer in the rail) - switch to alternate trigger on coil package, if necessary - replace coil package if neither trigger closes

If triggers test OK, they may not be getting sufficient pressure from the rolling wheel (e.g., the resilient foam under the coils is collapsing) - loosen the two nuts holding the coil package, raise it up, insert a nonferritic spacer (\approx 3-4 mm thick) between its horizontal plate and the magnet, lower it into place, and tighten nuts
2. Trigger but no signal
Check continuity of both transmitter and receiver coils with multimeter (at coil package or at end of track cable) - DC resistance should be 6-7 Ω . If either coil is broken (open) or shorted, replace coil package

Check that high voltage at analog box is ON

Check integrity of any exposed cables (rodents like to chew on them)

3. Noise on analog signal	Check that track cable shield connections to aluminum bracket of coil package and frame of analog electronics box - check that all BNC's are tight - use ground straps to connect frames of all boxes of electronics - install a power conditioner on 110 V power supply
4. Cuts at the outer edge of the coil package cover	Increase spacing between the edge of the coil package and the lip of the tapered recess by increasing the number of washers between the magnet nuts and the vertical plate.

FUTURE CONSIDERATIONS

1. To locate the reporting computer at a remote location, the RS-232 link with the digital electronics needs to be replaced with:
 - a. RS-422 or RS-485 link,
 - b. fiberoptic link,
 - c. telephone line with modems, or
 - d. microwave link.
2. The digital electronics can probably be repackaged into the empty module in the analog electronics rack.
3. The BNC connectors need to be replaced with a system that will be less subject to corrosion during long-term field use. Possibilities include simple twisted pairs with screw terminals, or more elaborate MIL-type connectors.
4. The coil package needs to be made weather-proof (or at least moisture-resistant). Currently, the resilient foam may absorb some water, and the several tapes inside will not withstand extensive exposure to moisture.
5. The Nd-Fe-B magnet needs a protective coat against rusting.
6. A method of wheel flagging other than sequence numbers will be necessary. Possibilities are video taping (as done by WHEELFAX), or firing paint pellets at the wheels.
7. It may be desirable to bury the analog and digital electronics in a shielded box next to the track to minimize the travel distance of rf and low-level signals.
8. One possible redesign of the in-rail transducer would give it a hard surface (highly resistant to wear) and have it ride on pivots or compression springs to accommodate the moving wheel. This would cut maintenance even further.

9. It will eventually be necessary to incorporate a switching mechanism that will sense a train as it approaches the inspection site and turn the equipment on.
10. Field experience may indicate some changes in the processing algorithm:
 - a. Do we need to adjust the echo/RT amplitude ratio of 20% for critical flaws?
 - b. Is three the right number at which to raise the multiple flaw flag?
 - c. Should the amplitude be adjusted for the distance the signal has traveled (as measured by its arrival time)? The first and second RT amplitudes can be used to measure the attenuation.
 - d. Is there any value to processing the flaw peaks between the first and second RTs?
11. The coil in Fig. 2 is presently hand-wound. We need to explore automated production for larger quantities.
12. Inspection of the wheels on both side of the train is obviously necessary, so test sites will be necessary in both tracks.
13. Since the "main bang" and round trip signals (Fig. 18A) mask about 20% of the potential flaw signals, it would require two sensors in the same track to assure 100% tread coverage. Locating the EMATs a quarter of a wheel circumference apart will prevent their blind spots from overlapping. It is also likely that a correlation of the analyses of the two probes would increase reliability.
14. Lightning will be a danger to this system. Nothing will protect against a strike directly on the transducer, but it would be desirable to isolate from pulses traveling along the rail from remote hits. The railroads are likely to have considerable experience with this problem.
15. The current software does not cover the wheel sizes used in locomotives. Should the electronic noise from the traction motors prove not to be too great so that good measurements are possible, this can easily be modified.
16. The trigger system that indicates the wheel is in position needs improvement for mechanical and electrical reliability. The most likely current candidate is a strain gage bridge on the rail web to sense the shear load as the wheel passes over the EMAT. Other possibilities include noncontact inductive sensors.
17. A hybrid system including these EMATs and other sensors (such as accelerometers) might provide an even more complete picture of wheel fitness.

OTHER POTENTIAL APPLICATIONS

The energy of Rayleigh waves is largely confined to the two dimensions of a surface as opposed to body waves that spread through three dimensions. The Rayleigh wave signal, therefore, attenuates as the square of the distance traveled, rather than the cube. In our early work, we saw as many as 18 round trips (p. 26) of the wheel circumference. This amounts to about 55 m (180 ft) total travel.

This long distance capability of the EMAT described in this report suggests the possibility of ultrasonic inspection of large scale structures where it would be difficult or time consuming to scan a probe near all potential surface cracks. For example, a single, linear sweep of the transducer would inspect the large steel panels used in the construction of ship hulls or chemical storage tanks. Since EMATs require no acoustic couplant and little or no surface preparation, they readily lend themselves to field use.

ACKNOWLEDGMENTS

A considerable number of people have been involved in this work in various ways and at various time.

From the FRA, Clifford Gannett, Claire Orth, and Donald Gray have all provided valuable guidance.

From TTC we received a great deal of help and cooperation in obtaining test wheels and rail sections. Of course, the field tests would have been impossible without their collaboration. Our main contact has been Robert Larson, Jr., who put a great deal of effort into this work. Some of the many others include Britto Rajkumar, Robert Vandeberg, Robert Florom, Alex Harrell, David Van Dyke, Daisy Cheng (summer intern), and several train and track crews.

We are indebted to John Cowan of The Fax Corp. in Danbury, Connecticut, Ansgar Wilbrand of IzFP in Saarbrücken, Germany, and Mike Giesking of Wheel Checkers in Denver, Colorado, for considerable background information.

Within our own lab, there have been many helpful ideas and considerable assistance at all stages. We are especially grateful to Dale Fitting, Todd McGuire, Christopher Fortunko, Daniel Vigliotti, and many others. Many of the public notices appearing in the Appendix are the result of efforts by Collier Smith.

APPENDIX: PUBLIC NOTICES

Our Public Information Office has disseminated several notices regarding this work. These were used in internal newsletters as well as several public periodicals. Some of this publicity has generated numerous inquiries from both potential users as well as those interested in possible commercial production.

Those public notices of which we are aware are:

1. "NBS Monthly Highlights," Feb. 1988, pp.3-4.
2. "NIST Monthly Highlights," Sept. 1989, pp. 2-3.
3. "Materials Evaluation," Sept. 1989, p. 1018.
4. "NIST Update," Jan.22, 1990, p. 3.
5. "Sensor Technology," March 1990, pp.4-5.
6. "Sensors," March 1990, pp. 12-13.
7. "Metalworking News," April 30, 1990.
8. "NIST Research Reports," May 1990, pp. 28-29.
9. "BusinessWeek," June 4, 1990, p. 95.
10. Frankfurter Allgemeine Zeitung, June 26, 1990.

The authors can provide copies to any interested parties.

BIBLIOGRAPHIC DATA SHEET

1. PUBLICATION OR REPORT NUMBER NISTIR 91-3967
2. PERFORMING ORGANIZATION REPORT NUMBER
3. PUBLICATION DATE May 1991

4. TITLE AND SUBTITLE

Report No. 22
TREAD CRACK DETECTION IN RAILROAD WHEELS:
AN ULTRASONIC SYSTEM USING EMATS

5. AUTHOR(S)

Raymond E. Schramm, Alfred V. Clark, Jr., Dragan V. Mitrakovic, Yossef Cohen, Peter J. Shull, Stephen R. Schaps

6. PERFORMING ORGANIZATION (IF JOINT OR OTHER THAN NIST, SEE INSTRUCTIONS)

U.S. DEPARTMENT OF COMMERCE
NATIONAL INSTITUTE OF STANDARDS AND TECHNOLOGY
BOULDER, COLORADO 80303-3328

7. CONTRACT/GRANT NUMBER

DTFR 53-89-X-00018

8. TYPE OF REPORT AND PERIOD COVERED

Final 9/85 - 12/90

9. SPONSORING ORGANIZATION NAME AND COMPLETE ADDRESS (STREET, CITY, STATE, ZIP)

U.S. Department of Transportation, Federal Railroad Administration, Office of Research and Development, Washington, DC 20590

10. SUPPLEMENTARY NOTES

11. ABSTRACT (A 200-WORD OR LESS FACTUAL SUMMARY OF MOST SIGNIFICANT INFORMATION. IF DOCUMENT INCLUDES A SIGNIFICANT BIBLIOGRAPHY OR LITERATURE SURVEY, MENTION IT HERE.)

This is report number 22 in a series covering research performed by the National Institute of Standards and Technology (NIST) for the Federal Railroad Administration (FRA). This report covers a project by the Materials Reliability Division (formerly the Fracture and Deformation Division) to develop and build an ultrasonic system to detect crack-type flaws in the tread of railroad wheels. To achieve fully automatic operation, the sensor is built into the rail so testing occurs as the train rolls past. Signal analysis takes place in real time.

The ultrasonic probe is an EMAT (electromagnetic-acoustic transducer). As configured here, the EMAT has a small footprint, and, due to its principle of operation, it does not require any acoustic couplant. The system operates in a pitch-catch mode. A short burst of Rayleigh (surface) waves travels around the wheel tread, and an echo indicates a flaw's presence and size. Testing was performed on both a short track in the NIST laboratory and the full-scale facilities of the Transportation Test Center (TTC) in Pueblo, Colorado.

This report documents the design, construction, and testing of the system. It is also to serve as an operational guide for the equipment being delivered to the FRA.

12. KEY WORDS (6 TO 12 ENTRIES; ALPHABETICAL ORDER; CAPITALIZE ONLY PROPER NAMES; AND SEPARATE KEY WORDS BY SEMICOLONS)

crack; EMAT; nondestructive testing; railroad wheel; roll-by inspection; ultrasonic

13. AVAILABILITY

UNLIMITED

FOR OFFICIAL DISTRIBUTION. DO NOT RELEASE TO NATIONAL TECHNICAL INFORMATION SERVICE (NTIS).

ORDER FROM SUPERINTENDENT OF DOCUMENTS, U.S. GOVERNMENT PRINTING OFFICE,
WASHINGTON, DC 20402.

ORDER FROM NATIONAL TECHNICAL INFORMATION SERVICE (NTIS), SPRINGFIELD, VA 22161.

14. NUMBER OF PRINTED PAGES

72

15. PRICE



